

Magnon-Magnon Interactions in O(3) Ferromagnets and Equations of Motion for Spin Operators

Slobodan M. Radošević*

Department of Physics, Faculty of Sciences, University of Novi Sad, Trg Dositeja Obradovića 4, Novi Sad, Serbia

The method of equations of motion for spin operators in the case of O(3) Heisenberg ferromagnet is systematically analyzed starting from the effective Lagrangian. It is shown that the random phase approximation and the Callen approximation can be understood in terms of perturbation theory for type B magnons. Also, the second order approximation of Kondo and Yamaji for one dimensional ferromagnet is reduced to the perturbation theory for type A magnons. An emphasis is put on the physical picture, i.e. on magnon-magnon interactions and symmetries of the Heisenberg model. Calculations demonstrate that all three approximations differ in manner in which the magnon-magnon interactions arising from the Wess-Zumino term are treated, from where specific features and limitations of each of them can be deduced.

Keywords: O(3) Heisenberg ferromagnet, Effective Field Theory, Wess-Zumino term, Hamiltonian lattice theory, Decoupling approximations

I. INTRODUCTION

The study of magnon-magnon interactions is a problem with long history [1] whose complexity initiated development of numerous analytical tools. Its importance goes far beyond pure academic interest since with the advent of new materials, especially those connected to the high-temperature superconductors [2–5], the question of magnon-magnon interactions and their influence on thermodynamic properties of ordered magnets became an urgent one to solve. This amounts not only to finding efficient calculation techniques, but also understanding how or why certain approximations work and what are their domains of applicability. With this in mind, it is useful to study simpler models [6]. In this case, they reveal some features generic to the wide class of spin systems otherwise concealed in more complicated ones containing second and third neighbor interaction, various types of frustration and anisotropies, random impurities etc. Much like 2D Ising model, due to several well established and exact results, the (quantum) O(3) Heisenberg ferromagnet has come to be a prototypical model for testing diverse theoretical and numerical methods.

Nearly all theories addressing the problem of magnon-magnon interactions are spin-operator oriented in the sense that all calculations are based on the operators used to define the Heisenberg model (See Fig. 1). The most straightforward way to incorporate the interaction effects is to express the localized spins in terms of bosonic/fermionic operators directly in the Heisenberg Hamiltonian or to use the coherent-state path integral (See e.g. [7, 8]). The original spin Hamiltonian is afterwards interpreted as describing the system of interacting bosons/fermions, to which standard perturbation theory, or suitable mean-field approximations (MFA), may be applied (See [1, 7–9] and references therein). Although techniques build upon boson/fermion representations of spin operators provide an important insight into the behavior of magnetic systems, they suffer from a universal disadvantage: The su(2) algebra of spin operators and

the dynamics of the spin system are fully satisfied only with exact boson/fermion Hamiltonian and corresponding Hilbert space. Accordingly, any approximation in the boson/fermion Hamiltonian, such as approximate expression for localized spins or some mean-field approximation, destroys the spin nature of (S^\pm, S^z) operators, often in an uncontrolled manner.

A different way to deal with magnon-magnon interactions is based on the equations of motion (EOM) for spin operators [10]. Aside from the fact that the EOM for spin operators are practically unsolvable for general Heisenberg-type Hamiltonian, the analysis through EOM gets more involved giving the fact that spin operators present basic dynamical variables and charge densities at the same time [11]. Despite all that, the method of equations of motion, especially in temperature-Green's function (TGF) disguise (See [12] for a recent review and original references), gained quite a popularity. There are several reasons for this. First, its predictions for thermodynamic properties of Heisenberg-type magnets agree with Monte Carlo simulations [12] and with experimental results (See e.g. [13–17] and references therein). Equally important is the flexibility of the method making it easily adjustable to systems with complex [18–22] or low-dimensional lattices [23–30], second and third-neighbor interaction or anisotropies [13, 15, 31–35], which is of great importance when studying real compounds. Also, the TGF method is recognized as useful in theories of diluted magnetic systems [36, 37], nuclear spin order in quantum wires [38], multiferroics models [39, 40] and even in theories of itinerant electron systems where Heisenberg Hamiltonian appears as an intermediate effective model [22, 41, 42]. The approximations made directly in the equations of motion, known as the decoupling schemes (DS) in the TGF jargon [12], enable one to solve linearized system of EOM-s thereby determining the magnon spectrum, correlation functions etc. By suitably choosing the parameters of linearization [43, 44], more or less satisfactory results may be obtained. Even though TGF method is extensively exploited in contemporary research (See the papers quoted earlier in this paragraph), a thorough discussion on EOM and magnon-magnon interactions seems to be lacking. This gap in the literature comes from the fact that the nonlinear Hamil-

* slobodan@df.uns.ac.rs

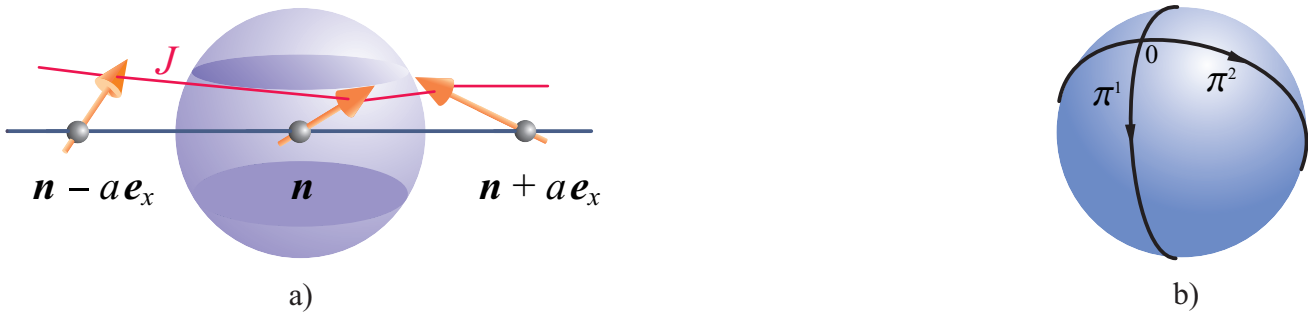


FIG. 1. Different perspectives on dynamical degrees of freedom and magnon-magnon interactions in $O(3)$ ferromagnets: a) In spin-operator-based approaches, interactions are viewed as a consequence of nontrivial algebra and Hilbert space of spin operators coupled through exchange integral J [One-dimensional lattice of localized $S = 1/2$ spins is displayed for clarity] b) In EFT, magnons are considered as a set of (local) coordinates on the sphere $S^2 = O(3)/O(2)$ and magnon-magnon interactions are dictated by the underlying geometry of S^2 , the non-Abelian character of $O(3)$ and the existence of conserved charges in ferromagnetic ground state.

tonian describing magnon-magnon interactions need not be introduced in EOM approach, which makes the comparison with usual boson/fermion representation theories rather difficult.

The brief sketch of boson/fermion representation and EOM for spin operators from two preceding paragraphs deliberately points on methodical differences in handling magnon-magnon interactions, as they appear to be among frequently used analytical tools and thus cover a significant part of approximate treatments of spin systems. Equally important, however, is their common feature: Being based on spin operators and not on the true degrees of freedom (i.e. magnons), these approximations tend to obscure the physics behind them. This is especially true for linearized EOM, since calculations are conducted without direct reference to magnon-magnon interaction operators.

An alternative view on magnons in a system of localized spins, based upon symmetry considerations, is put forward in [45]. As an extension of the phenomenological Lagrangian method [46–52] to the nonrelativistic systems, the outcome of [45] is the effective Lagrangian for the 3D $O(3)$ Heisenberg ferromagnet constructed from the magnon fields $\pi^1(x)$ and $\pi^2(x)$ transforming nonlinearly under $O(3)$ rotation group (The subject of nonlinear realizations and effective Lagrangians is reviewed in [53], while texts with special emphasis on nonrelativistic systems include [54–58]). The main advantage in viewing magnons as Goldstone bosons, accompanying $O(3) \rightarrow O(2)$ symmetry breakdown, is that their dynamics is completely separated from the $su(2)$ algebra of spin operators entering the Heisenberg Hamiltonian. Magnons are considered as local coordinates on $O(3)/O(2) = S^2$ and all information about magnon-magnon interactions are encoded in the nonlinear Lagrangian (See Fig. 1). The perturbative calculations may be conducted in a systematic manner, free of the upper mentioned ambiguities characterizing spin-operator oriented approaches. The general program of [45] is successfully applied on the calculation of the free energy up to two [59, 60] and three loops [61] and is subsequently extended to low dimensional ferromagnets [62–65]. If one

is concerned only with low-temperature series of the free energy and related quantities, which are strongly controlled by internal symmetry of the Heisenberg model, the continuum field-theoretic methods of [45, 56, 59–65] will suffice. However, the comparison with experimental data and other spin-operator-based methods often requires for the discrete symmetry of the lattice to be included also. This is the case, for example, with magnon energies whose dispersion deviates from simple k^2 law due to the lattice anisotropies. The symmetry of the lattice may be incorporated in the effective field description by the method of [66] (See also [56]), resulting in an effective theory which describes ferromagnet with the help of lattice magnon fields. This means that the internal $O(3)$ symmetry is implemented through the usual nonlinear realization (equivalently, symmetry may be realized linearly on the magnon fields, but with an additional nonlinear constraint), while the lattice symmetries enter via adequately chosen regulator. At the same time, the use of spatial lattice singles out canonical formalism in constructing quantum field-theoretic description of a ferromagnet. Beside the fact that the Hamiltonian lattice theory and the functional Lagrangian method with dimensional regularization yield the same results, as it was shown in [66], few other important issues favor canonical over functional integral formalism in this particular case. First, with the lattice magnon Hamiltonian at hand, a comparison with standard methods based on boson representations of the spin operators [1, 7, 8, 67, 68] becomes a much easier task. Second, EOM method (i.e. two-time temperature Green’s function theory) which is be systematically reexamined in present paper, is intimately related to the spin operator Hamiltonian through the definitions of thermodynamic averages. Also, the procedure of quantization itself is insightful regarding how magnon-magnon interactions may appear in an effective field theory. And finally, interacting Hamiltonian for ferromagnetic magnons, rather than the general form of interacting Lagrangian, reveals certain simplifications in loop calculations [66] if a Lagrangian contains the Wess-Zumino term.

The lattice Hamiltonian theory of magnon fields pro-

vides us with an efficient tool for studying effects of magnon-magnon interactions in O(3) ferromagnets, and likewise, the interactions induced by linearizations in EOM approach. This is an extremely important point since, according to the current understanding [12], the quality of DS can be judged only *a posteriori*. Also, it is difficult to distinguish between the true effects of magnon-magnon interactions induced by linearizations of EOM from pure artifacts of TGF formalism. All this can lead to incorrect interpretation of results obtained using EOM for spin operators. Previous remarks bring us to the main purpose of the present article. By explicitly identifying types of magnon-magnon interactions that actually constitute some of the well known DS and connecting them with internal symmetry of the O(3) ferromagnet, we put EOM approach in broader context of interacting spin waves and effective Lagrangians thereby connecting it with recent developments in these fields. At the same time we clarify some misinterpretations of EOM method in the case of O(3) ferromagnets. Quite generally, the effects of magnon-magnon interactions can be inferred either from low-temperature expansions of the free energy and related thermodynamic quantities or from renormalized magnon energies, as corresponding results in linear spin wave (LSW) approximation are well known [66]. Since the heart of EOM method lies in determination of the renormalized magnon energies, we shall concentrate on finding appropriate effective Lagrangian that yields, through the perturbation theory, desired magnon self-energy. This will allow us to determine the true nature of some well known linearizations from the physical point of view, i.e. relying only on magnon-magnon interactions and internal symmetry of the Heisenberg model.

The perturbation theory for lattice magnon fields shares many features with the standard effective field theory. The most important distinction concerns calculation details, as the spatial lattice replaces continuum field theoretic setting. Section II summarizes main definitions and relations needed for loop calculations which are presented in Sec. III and IV. Specifically, it is shown in Sec. III that the random phase approximation (RPA) and the Callen approximation (CA) can be understood as interaction theories for type B magnons (see [57, 69] for A/B classification of Goldstone fields). Finally, Sec. IV describes the second-order approximation of Kondo and Yamaji for one dimensional ferromagnet as a perturbation theory for type A magnons. Further justification of the lattice magnon field formalism comes from comparison with Quantum Monte Carlo simulation [sections III F and IV C 3] which, at the same time, supports some of our conclusion regarding RPA, CA and KYA.

II. LATTICE LAPLACIANS AND MAGNON-MAGNON INTERACTIONS

Conventional effective field theory (EFT) combines derivative and loop expansions to set up perturbative calculations to given order in some energy scale [53–55]. The relevant scale for ferromagnets is determined by temperature and EFT enables one to systematically calculate free

energy in powers of T [51, 59–65]. Yet, as emphasized in the Introduction, some issues concerning ordered magnets are adequately treated by the perturbation theory for lattice magnon fields which preserves the full symmetry of Heisenberg Hamiltonian. This approach, adjusted for O(3) ferromagnets and systematically exposed in following sections, includes couplings of neighboring sites through the lattice Laplacian. For general lattice it is defined by [70]

$$\nabla^2 \phi(\mathbf{x}) = \frac{2D}{Z_1 |\boldsymbol{\lambda}|^2} \sum_{\{\boldsymbol{\lambda}\}} \left[\phi(\mathbf{x} + \boldsymbol{\lambda}) - \phi(\mathbf{x}) \right], \quad (1)$$

where \mathbf{x} denotes a lattice site, D is the dimensionality of spatial lattice and $\{\boldsymbol{\lambda}\}$ are vectors connecting each lattice site with its Z_1 nearest neighbors. The definition (1) can be extended in an obvious manner to next-nearest neighbor couplings. The plane wave solutions, corresponding to free magnons, are built with eigenvalues of ∇^2

$$\begin{aligned} \nabla^2 \exp[i\mathbf{k} \cdot \mathbf{x}] &= -\frac{2D}{|\boldsymbol{\lambda}|^2} [1 - \gamma_D(\mathbf{k})] \exp[i\mathbf{k} \cdot \mathbf{x}] \quad (2) \\ &\equiv -\widehat{\mathbf{k}}^2 \exp[i\mathbf{k} \cdot \mathbf{x}], \quad \gamma_D(\mathbf{k}) = Z_1^{-1} \sum_{\{\boldsymbol{\lambda}\}} \exp[i\mathbf{k} \cdot \boldsymbol{\lambda}]. \end{aligned}$$

Depending the presymplectic structure [57, 69], Goldstone bosons may be classified as type A or B. In the present context, magnons of type A possess free energies proportional to $\widehat{\mathbf{k}}$ and those of type B to $\widehat{\mathbf{k}}^2$. As a consequence of derivative couplings, the loop integrals generally contain eigenvalues combining loop and external momenta, $\widehat{\mathbf{p} - \mathbf{q}}^2$. These can be simplified according to

$$\int_{\mathbf{q}} \langle n_{\mathbf{q}} \rangle_0 \widehat{\mathbf{p} - \mathbf{q}}^2 = \int_{\mathbf{q}} \langle n_{\mathbf{q}} \rangle_0 \left[\widehat{\mathbf{p}}^2 + \widehat{\mathbf{q}}^2 - \frac{|\boldsymbol{\lambda}|^2}{2D} \widehat{\mathbf{p}}^2 \widehat{\mathbf{q}}^2 \right] \quad (3)$$

where $\langle n_{\mathbf{p}} \rangle_0$ denotes Bose distribution for free magnons and

$$\int_{\mathbf{q}} \equiv \int_{\text{IBZ}} \frac{d^D \mathbf{q}}{(2\pi)^D}. \quad (4)$$

The focus in Sec. IV is on one dimensional ferromagnets described by an effective theory that includes couplings of lattice magnon fields spanning beyond nearest neighbors. To make presentation in Sec. IV more transparent, we shall denote with $\nabla_{(2)}^2$ the Laplacian for second neighbor couplings on a chain. It is defined by

$$\nabla_{(2)}^2 e^{iqx} = -\frac{1}{2a^2} [1 - \gamma(2q)] e^{iqx} \equiv -\widehat{2q}^2 e^{iqx}, \quad (5)$$

so that

$$\widehat{2q}^2 = \widehat{q}^2 \left[1 - \frac{a^2}{4} \widehat{q}^2 \right] \quad (6)$$

and $\gamma(q)$ is defined in (2) for $D = 1$. An analogue of (3) for $\nabla_{(2)}^2$ reads

$$\begin{aligned} \int_{\mathbf{q}} \langle n_{\mathbf{q}} \rangle_0 \widehat{2p - 2q}^2 &= \int_{\mathbf{q}} \langle n_{\mathbf{q}} \rangle_0 \left[\widehat{2p}^2 + \widehat{2q}^2 \right. \\ &\quad \left. - 2a^2 \widehat{2p}^2 \widehat{2q}^2 \right]. \quad (7) \end{aligned}$$

Equations from this section will be used throughout the paper for loop calculations, frequently without direct reference.

III. PERTURBATION THEORY FOR TYPE B MAGNONS

We introduce lattice magnon Hamiltonian and accompanying diagrammatic rules for type B magnons [57, 69] in this section. They will serve as a basic for the systematic investigation of several approximate treatments of magnon-magnon interactions in O(3) ferromagnets for $D \geq 3$.

A. Lattice magnon Hamiltonian

The starting point in an effective field description of a ferromagnet is the classical Lagrangian [45] (See also [71–73]) of the unit vector field $U^i := [U^1, U^2, U^3]^T \equiv [\boldsymbol{\pi}(x), U^3(x)]^T$ transforming linearly under O(3)

$$\mathcal{L}_{\text{eff}} = \Sigma \frac{\partial_t U^1 U^2 - \partial_t U^2 U^1}{1 + U^3} - \frac{F^2}{2} \partial_\alpha U^i \partial_\alpha U^i + \Sigma_\mu H U^3. \quad (8)$$

$\Sigma = NS/V$ is the spontaneous magnetization per unit volume at $T = 0\text{K}$, F is a constant, to be fixed latter, H is the external field and α refers to the spatial coordinates. We also recall that the Lagrangian (8) collects all magnon-magnon interactions up to \mathbf{p}^2 . Due to the non-vanishing charge densities in the ground state and the non-Abelian character of the O(3) rotational group, the effective Lagrangian contains appropriate Wess-Zumino (WZ) term. Being linear in temporal derivatives, WZ term is responsible for nonrelativistic dispersion of ferromagnetic magnons [45, 74, 75] and (8) describes the system of type-B Goldstone bosons [69]. In contrast to this well known fact, its influence in perturbation theory, i.e. in loop corrections to the magnon self-energy and the ferromagnet free energy, is not fully appreciated. The reason for this is that WZ term is practically invisible in approaches based on boson representations, dominating the literature on magnon-magnon interactions [1, 67, 68], since it is hidden inside the commutation relations of spin operators.

As outlined in the Introduction, we shall employ canonical formalism in constructing the quantum theory. We first note that the field describing physical magnons is complex [45, 59, 69], $\psi(x) = \sqrt{\Sigma/2}[\pi^1(x) + i\pi^2(x)]$, since the equation governing their dynamics is of a Schrödinger type. The standard canonical prescription [76] then yields the canonical momentum in the form $\Pi = 2i\psi/[1 + U^3]$, with $U^3 = \sqrt{1 - (2/\Sigma)\psi^\dagger\psi}$. This path towards consistent quantum theory is of course completely legitimate, but nonlinear connection between ψ^\dagger and Π sends important part of the magnon-magnon interactions from the Hamiltonian $\mathcal{H}(\psi, \psi^\dagger)$ to the canonical commutation relations, $[\psi(\mathbf{x}), \Pi(\mathbf{y})] = i\delta(\mathbf{x} - \mathbf{y})$. The quantum field theory of this sort is strongly reminiscent of the initial, spin-operator oriented, approach and is in fact something we would like to avoid. Fortunately, all complications concerning canonical commutation relations can be circumvented by noting that terms with single temporal derivative may be eliminated from the Lagrangian (8) with the help of the equation

of motion for $U(\mathbf{x}, t)$ [76] (See also [77]). In this manner, we obtain the free magnon Lagrangian (bilinear in magnon fields π^1 and π^2) and nonlinear part describing their interaction [66]. Canonical quantum interaction theory may be constructed starting from this Lagrangian. For the present purposes, we shall be needing terms up to and including eight magnon field operators. An straightforward calculation yields redesigned Hamiltonian [66]. This Hamiltonian, however, includes only magnon-magnon interactions of the order \mathbf{p}^2 . It is well known [49, 51, 52, 60, 61, 78] that consistent loop expansion must include interaction terms of higher order in magnon momenta. Following examples from Lorentz-invariant chiral perturbation theory [79, 80], we include higher order terms in momentum, i.e. in spatial derivatives, by putting the Hamiltonian on the (spatial) lattice. We find terms with four and eight magnon field operators

$$\begin{aligned} H_{\text{eff}} &= H_0 + H_{\text{int}}, \quad (9) \\ H_0 &= -\frac{1}{2m_0} v_0 \sum_{\mathbf{x}} \psi^\dagger(\mathbf{x}) \nabla^2 \psi(\mathbf{x}), \\ m_0 &= \frac{\Sigma}{2F^2}, \\ H_{\text{int}} &= H_4^{(a)} + H_4^{(b)} + H_8^{(a)} + H_8^{(b)}, \end{aligned}$$

where v_0 denotes the volume of the unit cell and

$$\begin{aligned} H_4^{(a)} &= \frac{F^2}{8} v_0 \sum_{\mathbf{x}} \boldsymbol{\pi}^2(\mathbf{x}) \boldsymbol{\pi}(\mathbf{x}) \cdot \nabla^2 \boldsymbol{\pi}(\mathbf{x}), \quad (10) \\ H_4^{(b)} &= -\frac{F^2}{8} v_0 \sum_{\mathbf{x}} \boldsymbol{\pi}^2(\mathbf{x}) \nabla^2 \boldsymbol{\pi}^2(\mathbf{x}), \end{aligned}$$

$$\begin{aligned} H_8^{(a)} &= -\frac{F^2}{128} v_0 \sum_{\mathbf{x}} [\boldsymbol{\pi}^2(\mathbf{x})]^3 \boldsymbol{\pi}(\mathbf{x}) \cdot \nabla^2 \boldsymbol{\pi}(\mathbf{x}), \\ H_8^{(b)} &= \frac{F^2}{128} v_0 \sum_{\mathbf{x}} [\boldsymbol{\pi}^2(\mathbf{x})]^2 \nabla^2 [\boldsymbol{\pi}^2(\mathbf{x})]^2, \quad (11) \end{aligned}$$

We have set $H = 0$ for the time being. In what follows, ψ will always be written to the right in expressions like $\boldsymbol{\pi} \cdot \boldsymbol{\pi}$. We also note that $\Sigma = S/v_0$ in a lattice theory, with S denoting the magnitude of localized spins. The LSW spectrum is fully recovered if we choose $F^2/\Sigma = JSZ_1|\boldsymbol{\lambda}|^2/(2D) = 1/(2m_0)$ [see equation (13) bellow]. This simple connection between parameters of the effective theory and those of original Heisenberg model is a consequence of the ferromagnetic ground state.

Some comments on interacting magnon Hamiltonian (9)-(11) are in order. We observe that magnon-magnon interactions come in two categories, distinguished by superscripts a and b in (10)-(11). While $H_4^{(b)}$ and $H_8^{(b)}$ are typical interaction terms for theories of unit vector fields, those containing operator $\boldsymbol{\pi}(\mathbf{x}) \cdot \nabla^2 \boldsymbol{\pi}(\mathbf{x})$, namely $H_4^{(a)}$ and $H_8^{(a)}$, describe the magnon-magnon interactions originating in WZ term. Thus, they are specific to the ferromagnetic system and careful treatment of the magnon-magnon interactions arising in WZ term is mandatory, if the correct description of a ferromagnet is to be expected. We shall come back to this point several times in the text. It can also be seen from (9) and (10) that $H_0 + H_4^{(a)} + H_4^{(b)}$

is quite similar to the Dyson-Maleev Hamiltonian [81–83]. Both the Dyson’s construction and the Maleev boson representation [84] yield magnon Hamiltonian equivalent to $H_0 + H_4^{(a)} + H_4^{(b)}$, but only the method based on the effective Lagrangian (9) traces $\pi^2(x)\pi(x) \cdot \nabla^2 \pi(x)$ interaction back to the WZ term. Finally, the Hamiltonian given in (9) and (10)–(11), being the Hamiltonian of true Goldstone fields, makes the weakness of magnon-magnon interactions at low momenta rather obvious. Thus, $1/S$ expansion, a usual starting point in theories based on boson representations and *a priori* justification for the weakness of magnon-magnon interactions [1, 7, 67, 68] is, in fact, unnecessary. The magnons interact weakly at low momenta irrespective of the spin magnitude S , and this is what actually makes the perturbation theory well defined [85] even for $S = 1/2$.

B. Diagrammatic description of magnon-magnon interactions

Before proceeding with concrete perturbation theory calculations, we pause to introduce a useful variant of Feynman diagrams [66]. It is particularly suited to the magnon Hamiltonian (9), but it can be easily adapted to other scalar field theories with derivative couplings. This method will allow us to systematically keep track of individual contributions in various magnon-magnon processes, which will turned out to be of great importance when comparing magnon perturbation theory with approximations in the equations of motion. To account for the eight-magnon vertices, we slightly modify the notations used in [66].

We shall denote with $\boxed{4(a)}$, $\boxed{4(b)}$, $\triangleleft 8(a) \triangleright$ and $\triangleleft 8(b) \triangleright$ the vertices corresponding to interaction terms from (10)–(11). Depending on the structure of the vertex, lattice Laplacians may act on one, two or four magnon propagators. Apart from simplest, one-vertex diagrams, higher order corrections will always contain at least two lattice Laplacians acting on propagators. The calculations soon become quite involved, since the number of propagators, as well as the number of lattice Laplacians acting upon them, increases. To make them feasible, we associate with each vertex a color so that the vertex and the propagators affected by its lattice Laplacian are drawn using that color. The rest of the lines are sim-

ply drawn black. We label each propagator with $D + 1$ dimensional momentum $k := [\mathbf{k}, \omega_n]^T$ and the colored ones also carry $-\widehat{\mathbf{k}}^2$. Here $-\widehat{\mathbf{k}}^2$ denotes the eigenvalue of the lattice Laplacian, defined in (2), and $\omega_n = 2\pi nT$ are the Matsubara frequencies. When colored line passes through the vertex, the momentum in $-\widehat{\mathbf{k}}^2$ corresponds to algebraic sum of the incoming and outgoing momenta. If more than one Laplacian acts on a certain propagator, the line will carry one color for each vertex. We shall adopt the following convention on colored propagators belonging to a closed loop: If the lattice Laplacian of $\boxed{4(a)}$ or $\triangleleft 8(a) \triangleright$ acts on a magnon propagator closing a loop around it, the line will be drawn half-colored. When the Laplacian comes from $\boxed{4(b)}$ or $\triangleleft 8(b) \triangleright$, the line will be drawn in full color if the Laplacian acts on both contracted magnon field operators. Otherwise, the line will also be drawn half-colored. With this conventions we generalize the method of [66] to interacting terms with more than four magnon operators. The diagrams with colored lines and vertices will be referred to as the colored contractions. Later, in Sec. IV, we shall allow more than one Laplacian per vertex. Lastly, the magnon propagator and the free one-magnon energies for type B magnons are given by

$$D(\mathbf{x} - \mathbf{y}, \tau_x - \tau_y) \equiv \langle \text{T} \{ \psi(\mathbf{x}, \tau_x) \psi^\dagger(\mathbf{y}, \tau_y) \} \rangle_0 \quad (12)$$

$$= \frac{1}{\beta} \sum_{n=-\infty}^{\infty} \int_{\mathbf{q}} \frac{e^{i\mathbf{q} \cdot (\mathbf{x} - \mathbf{y}) - i\omega_n(\tau_x - \tau_y)}}{\omega_0(\mathbf{q}) - i\omega_n},$$

$$\omega_0(\mathbf{q}) = \frac{\widehat{\mathbf{q}}^2}{2m_0}, \quad (13)$$

and $\beta^{-1} \sum_n [\omega_0(\mathbf{p}) - i\omega_n]^{-1} = \langle n_{\mathbf{p}} \rangle_0$, where $\langle n_{\mathbf{p}} \rangle_0$ denotes Bose distribution for free magnons.

As an explicit example, consider a three-loop correction to the magnon self-energy arising from $H_8^{(b)}$. Formally, it is represented by

$$\Sigma_8^{(b)}(\mathbf{k}) = \text{---} \triangleleft 8(b) \triangleright \text{---} \quad (14)$$

Several colored contractions contribute to this particular diagram. These are

$$\text{---} \triangleleft 8(b) \triangleright \text{---} + \text{---} \triangleleft 8(b) \triangleright \text{---} = -\frac{4}{S^3} \frac{\langle n_x \rangle}{2m_0} v_0^2 \int_{\mathbf{Q}, \mathbf{q}} \langle n_{\mathbf{Q}} \rangle_0 \langle n_{\mathbf{q}} \rangle_0 \widehat{\mathbf{Q} - \mathbf{q}}^2, \quad (15)$$

$$\text{diagram 1} + \text{diagram 2} = -\frac{4}{S^3} \frac{\langle n_{\mathbf{x}} \rangle^2}{2m_0} v_0 \int_{\mathbf{q}} \langle n_{\mathbf{q}} \rangle_0 \widehat{\mathbf{k} - \mathbf{q}}^2, \quad (16)$$

$$\text{diagram 1} + \text{diagram 2} = -\frac{2}{S^3} \frac{v_0^3}{2m_0} \int_{\mathbf{q}, \mathbf{p}, \mathbf{Q}} \langle n_{\mathbf{q}} \rangle_0 \langle n_{\mathbf{p}} \rangle_0 \langle n_{\mathbf{Q}} \rangle_0 \widehat{\mathbf{p} + \mathbf{q} - \mathbf{Q} - \mathbf{k}}^2 \quad (17)$$

since two colored loops closed around single vertex, as well as single colored closed loop with two colored external lines, vanish due to momentum conservation:

$$\text{diagram 1} = \text{diagram 2} = 0. \quad (18)$$

This is the analog of vanishing one-loop colored diagram of $H_4^{(b)}$ [66]. In the equations above $\langle n_{\mathbf{x}} \rangle = v_0 \int_{\mathbf{q}} \langle n_{\mathbf{q}} \rangle_0$ is the mean number of magnons per lattice site. Further examples, including three-loop corrections to self-energy from $H_4^{(a)}$ and $H_4^{(b)}$, can be found in [66]. Also, following [66], we omit combinatorial factors in front of diagrams and include them directly in corresponding equations. For example, each of colored contractions from equation (15) is accompanied by a combinatorial factor of

16, which is just the number of permutations of black and colored propagators which leave the diagram unchanged. We note one, more or less obvious, fact concerning one-vertex diagrams: the number of closed loops equals the number of $\langle n_{\mathbf{q}} \rangle_0$'s. This can easily be checked by inspection of the equations (15)-(17).

C. Two-loop correction to the magnon self-energy

To calculate the two-loop correction to the magnon self-energy, one must include magnon-magnon interactions described by $H_4^{(a)}$ and $H_4^{(b)}$. A direct computation shows that one-vertex diagrams, as well as two-vertex diagrams with both external lines attached to the same vertex, simply renormalize the magnon mass [86] ($m_0 \rightarrow m(T)$), while the "sunset" diagrams (each vertex carrying single external and three internal lines) change the geometry of the magnon dispersion. The result is [66]

$$\begin{aligned} \Sigma(\mathbf{k}, i\omega_n) &= \frac{\widehat{\mathbf{k}}^2}{2m_0} [A(T) + A(T)B(T)] + \frac{\widehat{\mathbf{k}}^2}{2m_0} \frac{1}{2S^2} \left(\frac{|\boldsymbol{\lambda}|^2}{2D} \right)^2 \frac{v_0^2}{2m_0} \int_{\mathbf{p}, \mathbf{q}} F_{\mathbf{p}, \mathbf{q}}^{\mathbf{k}}(i\omega_n) \widehat{\mathbf{q}}^2 \left(\widehat{\mathbf{p}}^2 + \widehat{\mathbf{k}}^2 \right) \left(\widehat{\mathbf{q}}^2 - \widehat{\mathbf{p} - \mathbf{q}}^2 \right), \\ F_{\mathbf{p}, \mathbf{q}}^{\mathbf{k}}(i\omega_n) &= \frac{\langle n_{\mathbf{p}} \rangle_0 [1 + \langle n_{\mathbf{q}} \rangle_0 + \langle n_{\mathbf{k} + \mathbf{p} - \mathbf{q}} \rangle_0] - \langle n_{\mathbf{q}} \rangle_0 \langle n_{\mathbf{k} + \mathbf{p} - \mathbf{q}} \rangle_0}{\omega_0(\mathbf{k} + \mathbf{p} - \mathbf{q}) - \omega_0(\mathbf{p}) + \omega_0(\mathbf{q}) - i\omega_n}, \\ A(T) &= \frac{1}{S} \frac{|\boldsymbol{\lambda}|^2}{2D} v_0 \int_{\mathbf{q}} \langle n_{\mathbf{q}} \rangle_0 \widehat{\mathbf{q}}^2, \\ B(T) &= \frac{1}{S} \frac{1}{2m_0 T} \frac{|\boldsymbol{\lambda}|^2}{2D} v_0 \int_{\mathbf{p}} \frac{\langle n_{\mathbf{p}} \rangle_0 [\langle n_{\mathbf{p}} \rangle_0 + 1]}{T} [\widehat{\mathbf{p}}^2]^2, \end{aligned} \quad (19)$$

where $F_{\mathbf{p}, \mathbf{q}}^{\mathbf{k}}(i\omega_n)$ comes from the Matsubara summation in the sunset diagram, and $\langle n_{\mathbf{p}} \rangle_0 [\langle n_{\mathbf{p}} \rangle_0 + 1]/T$ is induced by two-loop diagrams in which both external lines are attached to the same vertex (See [66]). Renormalized magnon energies are now easily found as $\omega_{2\text{loop}}(\mathbf{k}) = \omega_0(\mathbf{k}) - \delta\omega_{2\text{loop}}(\mathbf{k})$, with $\delta\omega_{2\text{loop}}(\mathbf{k}) = \lim_{\delta \rightarrow 0} \text{Re}\Sigma(\mathbf{k}, \omega_0(\mathbf{k}) + i\delta)$. It is seen that magnons, as pions in Lorentz-invariant theories [79, 87], remain gap-

less at two loop. In the rest of this section we shall exploit perturbation theory to test certain approximate treatments of magnon-magnon interactions against two-loop result (19). The calculation that led to (19) will be referred to as true magnon interaction theory, since it preserves spin-rotation symmetry up to and including two-loop corrections to the magnon self-energy.

D. The Random Phase Approximation

This well known approximation [12] is usually described as the one in which correlations between S^z and S^\pm operators from adjacent sites are neglected. Though it is most frequently discussed within TGF formalism, it can be easily obtained by replacing $S_{\mathbf{x}}^z(t)$ with site-independent average $\langle S^z \rangle$ in the equations of motion and commutation relations for $S_{\mathbf{x}}^\pm(t)$. The net effect of this approximation is the renormalization of magnon mass, $m_0 \rightarrow m_0 \times S/\langle S^z \rangle$, leading to incorrect description of thermodynamics at low temperatures (the presence of so-called spurious T^3 term in low-temperature series for spontaneous magnetization). It should be obvious from renormalized magnon spectrum and low-temperature series of spontaneous magnetization that RPA transforms localized interacting spins into a system of lattice bosons, as one can introduce Schrödinger field operators $[\psi(\mathbf{x}, t), \psi^\dagger(\mathbf{y}, t)] = v_0 \Delta(\mathbf{x} - \mathbf{y})$, in terms of which

$$S_{\mathbf{x}}^+(t) \stackrel{\text{RPA}}{\equiv} \sqrt{2\langle S^z \rangle} \psi(x), \quad S_{\mathbf{x}}^-(t) \stackrel{\text{RPA}}{\equiv} \sqrt{2\langle S^z \rangle} \psi^\dagger(x),$$

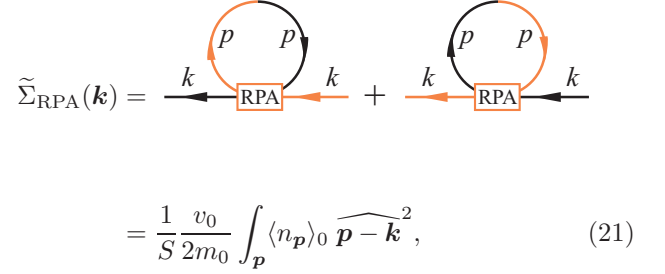
$$\omega_{\text{RPA}}(\mathbf{k}) = \frac{\hat{\mathbf{k}}^2}{2m_{\text{RPA}}}, \quad m_{\text{RPA}} = m_0 \frac{S}{\langle S^z \rangle}, \quad (20)$$

and the RPA description of O(3) HFM formally corresponds to the free field solution of this bose theory. For example, the correlation function $\langle S_{\mathbf{x}}^- S_{\mathbf{x}}^+ \rangle$ can be written as $\langle S_{\mathbf{x}}^- S_{\mathbf{x}}^+ \rangle_{\text{RPA}} = 2\langle S^z \rangle v_0 \langle \psi^\dagger(\mathbf{x}) \psi(\mathbf{x}) \rangle_{\text{RPA}} = 2\langle S^z \rangle v_0 \int_{\mathbf{k}} \langle n_{\mathbf{k}} \rangle_{\text{RPA}}$, where $\langle n_{\mathbf{k}} \rangle_{\text{RPA}}$ denotes the Bose distribution for magnons with energies $\omega_{\text{RPA}}(\mathbf{k})$. This agrees with standard TGF theory [12]. Much less trivial is the question of magnon-magnon interactions induced by RPA.

After original papers of Tyablikov and Bogolyubov, a number of authors [88–92] succeeded in obtaining the same results using different techniques. Where they all had failed is to connect RPA results with magnon-magnon interactions and internal symmetry of the model, since all those works (including the original one of Tyablikov and Bogolyubov) are spin-operator oriented. In particular, the perturbation theory in [89, 90, 92] is built on convenient MFA and fermion representation of spin operators, respectively, while [88, 91] develop linked cluster and $1/Z$ expansion.

It is only recently [66] suggested that RPA can be obtained in physically more transparent manner, using the perturbation theory for lattice magnon fields. The approximation in question is the replacement of $H_{\text{eff}} = H_0 + H_4^{(a)} + H_4^{(b)}$ with $H_{\text{RPA}} = H_0 - H_4^{(b)}$, leading to the model in which magnon-magnon interactions specific to the model with a WZ term are omitted (see [66] for details). The one-loop self energy in this approximation

can be written as



$$\tilde{\Sigma}_{\text{RPA}}(\mathbf{k}) = \text{diagram 1} + \text{diagram 2} = \frac{1}{S} \frac{v_0}{2m_0} \int_{\mathbf{p}} \langle n_{\mathbf{p}} \rangle_0 \widehat{\mathbf{p} - \mathbf{k}}^2, \quad (21)$$

where $\boxed{\text{RPA}} = -\boxed{4(b)}$ denotes the corresponding vertex. Of course, this cannot be the final result, since (21) implies the gap in magnon spectrum. To get physically acceptable self-energy, we must impose the constrain $\tilde{\mathcal{I}} := v_0 \int_{\mathbf{p}} \langle n_{\mathbf{p}} \rangle_0 \hat{\mathbf{p}}^2 = 0$. But this is equivalent to $v_0 \int_{\mathbf{p}} \langle n_{\mathbf{p}} \rangle_0 \gamma(\mathbf{p}) = v_0 \int_{\mathbf{p}} \langle n_{\mathbf{p}} \rangle_0 \equiv \langle n_{\mathbf{x}} \rangle$, and the constrain actually introduces site-independent mean number of magnons, resembling the replacement of the operator $S_{\mathbf{x}}^z(t)$ with site-independent average $\langle S^z \rangle$ in TGF theory. Renormalized magnon energies become

$$\omega_{\text{RPA}}(\mathbf{k}) = \omega_0(\mathbf{k}) - \Sigma_{\text{RPA}}(\mathbf{k}) = \frac{\hat{\mathbf{k}}^2}{2m_0} \frac{S - \langle n_{\mathbf{x}} \rangle}{S}, \quad (22)$$

which is indeed the low-temperature limit of RPA result. If we reverse the steps leading us to the effective Hamiltonian of lattice magnon fields, we see that RPA can be taught of as arising from the effective Lagrangian

$$\mathcal{L}_{\text{eff}}^{\text{RPA}} = \frac{\Sigma}{2} (\partial_t U^1 U^2 - \partial_t U^2 U^1) - \frac{F^2}{2} \partial_\alpha U^i \partial_\alpha U^i - \frac{F^2}{4} \pi^2(\mathbf{x}) \Delta \pi^2(\mathbf{x}). \quad (23)$$

which manifestly violates internal O(3) symmetry of the Heisenberg spin Hamiltonian starting at $\mathcal{O}(\mathbf{p}^2)$. We stress that the reduction of magnon-magnon interactions is crucial for thermodynamics of O(3) ferromagnets, for spurious terms in low-temperature series for free energy are present whether or not the constrain $v_0 \int_{\mathbf{p}} \langle n_{\mathbf{p}} \rangle_0 \hat{\mathbf{p}}^2 = 0$ is implemented [66].

As noted in the Introduction, RPA is widely used tool for studying magnetic systems [12–28, 31–42]. Thus, to be able to correctly interpret results obtained from RPA, it is of interest to fully grasp the approximation in itself. The spin operator-based mathematical machinery of two-time temperature Green's functions makes the physics involved less obvious, and this can lead to a wrong conclusion. For instance, the authors of a recent paper [93] characterize RPA as a theory which "which does not take account of spin correlations or magnon-magnon interactions". This is at best misleading, since we have shown that RPA corresponds to an effective field theory in which magnon-magnon interactions arising in the WZ term are omitted, but those induced by the unimodular constraint are kept. Thus, the difference between LSW and RPA comes from magnon-magnon interactions described by $-H_4^{(b)}$ of (10). The thermodynamic averages in RPA are actually calculated using $H_{\text{RPA}} = H_0 - H_4^{(b)}$ and not the full Heisenberg Hamiltonian, as one may expect from the mathematical formalism of TGF theory [12, 94].

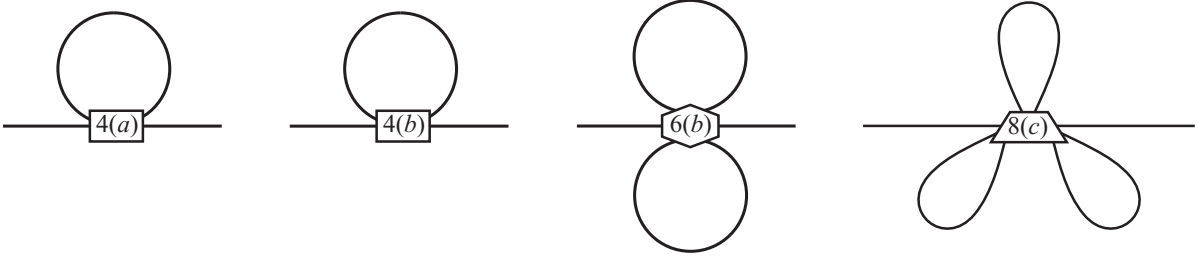


FIG. 2. The diagrams constituting magnon self-energy in the Callen approximation.

E. The Callen Approximation

1. Magnon Spectrum

Next we consider the Callen approximation (CA) (See [12] and references therein), which may also be viewed as a linearization scheme for EOM of spin operators. The Callen's linearization approximately accounts for the short-range fluctuations of the order parameter, apparently neglected in RPA. As a result of CA, magnons acquire renormalized mass

$$m_{\text{CA}}^{-1} = m_{\text{RPA}}^{-1} \left[1 + 2 \frac{\langle S^z \rangle}{2S^2} v_0 \int_{\mathbf{q}} \langle n_{\mathbf{q}} \rangle_{\text{CA}} \gamma(\mathbf{q}) \right], \quad (24)$$

with unchanged geometry of dispersion relation

$$\omega_{\text{CA}}(\mathbf{k}) = \frac{\hat{\mathbf{k}}^2}{2m_{\text{CA}}}. \quad (25)$$

$\langle S^z \rangle / 2S^2$, usually denoted as $\alpha(T)$, is a phenomenological parameter introduced by Callen to get a "correction to RPA" [95] ($\alpha(T) = 0$ directly leads to RPA). Since the discussion from previous section pointed out on the neglect of magnon-magnon interactions generated by WZ term as a defining feature of RPA, the question of magnon-magnon interactions induced by CA naturally arises. Now we examine it in detail.

First, we observe that the entire effect of Callen's linearization again reduces to the pure renormalization of magnon mass. This means that the magnon-magnon interactions are described solely by one-vertex interactions (perturbations), i.e. sunset and other similar diagrams are absent as in the case of RPA. Further, using $\langle S^z \rangle \approx S - \langle n_{\mathbf{x}} \rangle$ which is certainly good approximation at low temperatures, we see that m_{CA}^{-1} contains terms linear, quadratic and cubic in $\langle n_{\mathbf{q}} \rangle$. According to the general structure of one-vertex corrections to the self-energy outlined in Sec. III, the effective Hamiltonian that ought to produce (25) through perturbation theory must contain terms with six magnon operators. However, they are absent from (9), since products of six magnon operators originating from term with spatial derivatives and WZ term precisely cancel. This is a special characteristic of the effective Lagrangian (8), and terms with six Goldstone fields generally appear in Lorentz-invariant theories [51, 79]. The most general effective Hamiltonian with six magnon field operator and single lattice derivative is

$$H_6 = H_6^{(a)} + H_6^{(b)} + H_6^{(c)} \quad (26)$$

with

$$\begin{aligned} H_6^{(a)} &= A_6 F^2 v_0 \sum_{\mathbf{x}} [\pi^2(\mathbf{x})]^2 \pi(\mathbf{x}) \cdot \nabla^2 \pi(\mathbf{x}), \\ H_6^{(b)} &= B_6 F^2 v_0 \sum_{\mathbf{x}} [\pi^2(\mathbf{x})]^2 \nabla^2 \pi^2(\mathbf{x}), \\ H_6^{(c)} &= C_6 F^2 v_0 \sum_{\mathbf{x}} \pi^2(\mathbf{x}) \pi(\mathbf{x}) \cdot \nabla^2 [\pi(\mathbf{x}) \pi^2(\mathbf{x})], \end{aligned} \quad (27)$$

where A_6, B_6 and C_6 are arbitrary constants. We can safely choose $C_6 = 0$, since this kind of interaction is not generated neither by $\partial_\alpha \mathbf{U} \cdot \partial_\alpha \mathbf{U}$, nor by WZ term of (8). Also, we may set $A_6 = 0$ as the the contribution of $H_6^{(a)}$ to the self-energy

$$\begin{aligned} \Sigma_6^{(a)}(\mathbf{k}) &= \text{diagram 6(a)} + \text{diagram 6(a)} \quad (28) \\ &= \frac{48A \langle n_{\mathbf{x}} \rangle^2}{S^2} \frac{\hat{\mathbf{k}}^2}{2m_0} + \frac{96A \langle n_{\mathbf{x}} \rangle}{S^2} \frac{v_0}{2m_0} \int_{\mathbf{q}} \langle n_{\mathbf{q}} \rangle_0 \hat{\mathbf{q}}^2 \end{aligned}$$

contains the term $\propto \hat{\mathbf{k}}^2 \langle n_{\mathbf{x}} \rangle^2 S^{-2}$, which does not appear in $\omega_{\text{CA}}(\mathbf{k})$. As in earlier sections, diagram 6(a) denotes the corresponding vertex.

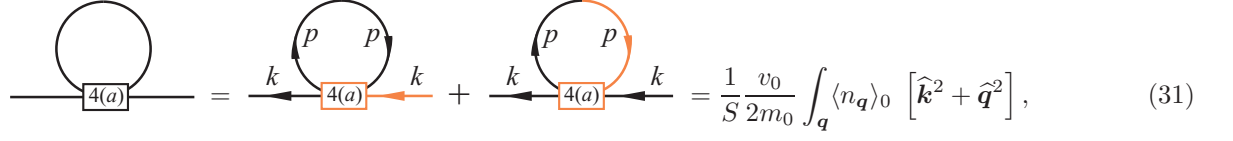
As far as eight-magnon terms are concerned, one easily verifies that $H_8^{(a)}$ and $H_8^{(b)}$ can not produce desired terms in magnon self-energy. The corrections arising from $H_8^{(b)}$ are listed in (15)-(17), revealing redundant contribution from (17). Also, $H_8^{(a)}$ gives unacceptable term $\propto \hat{\mathbf{k}}^2 \langle n_{\mathbf{x}} \rangle^3 S^{-3}$. In fact, the only way to reproduce $\omega_{\text{CA}}(\mathbf{k})$ through the perturbation theory is to include the new eight-magnon term

$$H_8^{(c)} = C_8 F^2 v_0 \sum_{\mathbf{x}} [\pi^2(\mathbf{x})]^3 \nabla^2 \pi^2(\mathbf{x}). \quad (29)$$

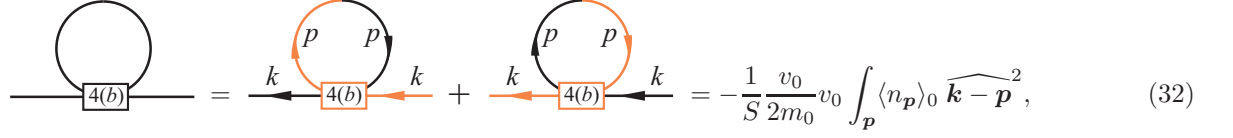
If the remaining coefficients from (27) and (29) are chosen to be $B_6 = 1/32$ and $C_8 = -1/576$, the Hamiltonian

$$H_{\text{CA}} = H_0 + H_4^{(a)} + H_4^{(b)} + H_6^{(b)} + H_8^{(c)}, \quad (30)$$

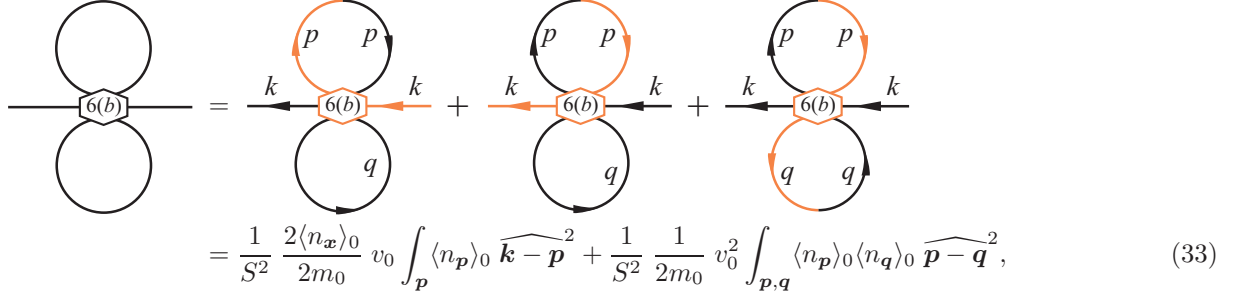
with suitable constrain on self-energy, yields $\omega_{\text{CA}}(\mathbf{k})$ through the perturbative corrections. To confirm this, we simply evaluate the one-vertex self-energy for diagrams depicted at Fig. 2. Since



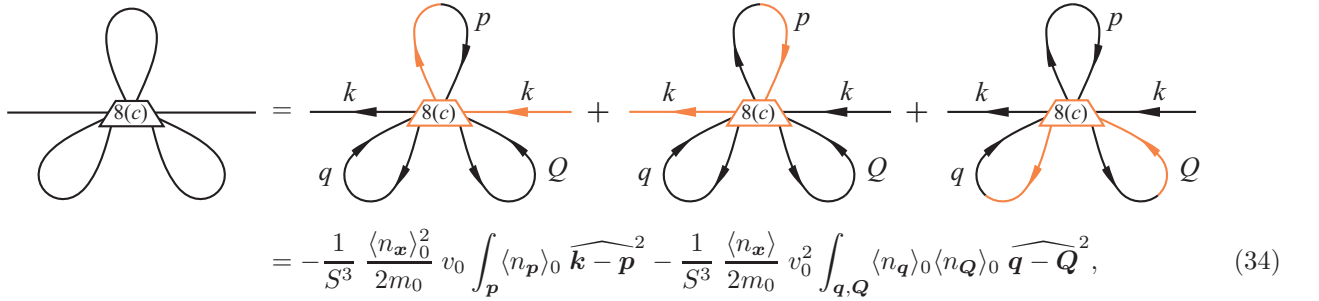
$$\text{Diagram 4(a)} = \text{Diagram 4(a)} + \text{Diagram 4(a)} = \frac{1}{S} \frac{v_0}{2m_0} \int_{\mathbf{q}} \langle n_{\mathbf{q}} \rangle_0 [\widehat{\mathbf{k}}^2 + \widehat{\mathbf{q}}^2], \quad (31)$$



$$\text{Diagram 4(b)} = \text{Diagram 4(b)} + \text{Diagram 4(b)} = -\frac{1}{S} \frac{v_0}{2m_0} v_0 \int_{\mathbf{p}} \langle n_{\mathbf{p}} \rangle_0 \widehat{\mathbf{k} - \mathbf{p}}^2, \quad (32)$$



$$\text{Diagram 6(b)} = \text{Diagram 6(b)} + \text{Diagram 6(b)} + \text{Diagram 6(b)} = \frac{1}{S^2} \frac{2\langle n_{\mathbf{x}} \rangle_0}{2m_0} v_0 \int_{\mathbf{p}} \langle n_{\mathbf{p}} \rangle_0 \widehat{\mathbf{k} - \mathbf{p}}^2 + \frac{1}{S^2} \frac{1}{2m_0} v_0^2 \int_{\mathbf{p}, \mathbf{q}} \langle n_{\mathbf{p}} \rangle_0 \langle n_{\mathbf{q}} \rangle_0 \widehat{\mathbf{p} - \mathbf{q}}^2, \quad (33)$$



$$\text{Diagram 8(c)} = \text{Diagram 8(c)} + \text{Diagram 8(c)} + \text{Diagram 8(c)} = -\frac{1}{S^3} \frac{\langle n_{\mathbf{x}} \rangle_0^2}{2m_0} v_0 \int_{\mathbf{p}} \langle n_{\mathbf{p}} \rangle_0 \widehat{\mathbf{k} - \mathbf{p}}^2 - \frac{1}{S^3} \frac{\langle n_{\mathbf{x}} \rangle_0}{2m_0} v_0^2 \int_{\mathbf{q}, \mathbf{Q}} \langle n_{\mathbf{q}} \rangle_0 \langle n_{\mathbf{Q}} \rangle_0 \widehat{\mathbf{q} - \mathbf{Q}}^2, \quad (34)$$

by putting all contributions together, we find:

$$\begin{aligned} \tilde{\Sigma}_{\text{CA}}(\mathbf{k}) &= \frac{1}{S} \frac{\widehat{\mathbf{k}}^2}{2m_0} \frac{|\lambda|^2}{2D} v_0 \int_{\mathbf{q}} \langle n_{\mathbf{q}} \rangle_0 \widehat{\mathbf{q}}^2 + \frac{\langle n_{\mathbf{x}} \rangle_0}{S^2} \frac{\widehat{\mathbf{k}}^2}{2m_0} v_0 \int_{\mathbf{q}} \langle n_{\mathbf{q}} \rangle_0 \gamma(\mathbf{q}) \left[2 - \frac{\langle n_{\mathbf{x}} \rangle_0}{S} \right] \\ &+ \frac{1}{S^2} \left[4\langle n_{\mathbf{x}} \rangle_0 - \frac{|\lambda|^2}{2D} \tilde{\mathcal{I}} \right] \frac{\tilde{\mathcal{I}}}{2m_0} - \frac{\langle n_{\mathbf{x}} \rangle_0}{S^3} \left[3\langle n_{\mathbf{x}} \rangle_0 - \frac{|\lambda|^2}{2D} \tilde{\mathcal{I}} \right] \frac{\tilde{\mathcal{I}}}{2m_0}, \end{aligned} \quad (35)$$

where, as in the case of RPA, $\tilde{\mathcal{I}} = v_0 \int_{\mathbf{q}} \langle n_{\mathbf{q}} \rangle_0 \widehat{\mathbf{q}}^2$. The absence of external momentum in terms proportional to $\tilde{\mathcal{I}}$ and $\tilde{\mathcal{I}}^2$ makes the self-energy (35) unphysical. These arise from two and three loop corrections that don't include true interactions generated by WZ term and unimodular constrain thus explicitly breaking O(3) symmetry at six and eight magnon field operators (see equations (44)-(46) below). Therefore, the contributions to the self energy calculated with $H_6^{(b)}$ and $H_8^{(c)}$ must be supplemented with additional constrain $\tilde{\mathcal{I}} = 0$ for a magnon spectrum to display the Goldstone mode. With restrictions on $\tilde{\mathcal{I}}$, the self-energy (35) reduces to

$$\Sigma_{\text{CA}}(\mathbf{k}) = \frac{\widehat{\mathbf{k}}^2}{2m_0} \left[\frac{\langle n_{\mathbf{x}} \rangle_0}{S} - \frac{\mathcal{I}}{S} + \frac{2\langle n_{\mathbf{x}} \rangle_0 \mathcal{I}}{S^2} - \frac{\mathcal{I} \langle n_{\mathbf{x}} \rangle_0^2}{S^3} \right], \quad (36)$$

where $\mathcal{I} = v_0 \int_{\mathbf{q}} \langle n_{\mathbf{q}} \rangle_0 \gamma_D(\mathbf{q})$. The magnon energies in this

approximation read

$$\begin{aligned} \omega_{\text{CA}}(\mathbf{k}) &= \frac{\widehat{\mathbf{k}}^2}{2m_0} - \Sigma_{\text{CA}}(\mathbf{k}) \\ &= \frac{\widehat{\mathbf{k}}^2}{2m_0} \frac{S - \langle n_{\mathbf{x}} \rangle_0}{S} \left[1 + \frac{S - \langle n_{\mathbf{x}} \rangle_0}{S^2} \mathcal{I} \right] \end{aligned} \quad (37)$$

and we recognize (37) as low-energy limit of Callen's result (25). From the point of view of an effective theory, all terms in magnon self energy arising from symmetry-violating parts of the magnon Hamiltonian must be constrained with $\tilde{\mathcal{I}} = 0$ to mimic O(3)-invariant perturbation theory. It is well known that fine tunings of this sort are a necessity if the approximation in question is too crude to encapsulate fundamental properties of a model under study [96]. In the present case it is the replacement of the lattice magnon Hamiltonian (9) with (30) that destroys spin-rotational invariance and affects the

magnon self-energy (35). Note, however, that the constrain $\tilde{\mathcal{I}} = 0$ should not be enforced on leading term in (35), since $H_4^{(a)} + H_4^{(b)}$ preserves spin-rotational invariance at four magnon operators. In contrast to RPA, the constrain $\tilde{\mathcal{I}} = 0$ merely eliminates the gap and should not be interpreted as introducing the site-independent number of magnons.

Thus, Callen's modification of RPA actually consists in adding three more interacting terms to H_{RPA} . The one with four magnon fields ($H_4^{(a)}$) carries interactions generated by the WZ term and preserves spin-rotational invariance up to one-loop corrections to the self energy. On the other hand, $H_6^{(b)}$ and $H_8^{(c)}$ describe additional interactions which are, however, not generated by the effective Lagrangian (8), as seen from (10)-(11). The differences between $\Sigma_{\text{CA}}(\mathbf{k})$, $\Sigma_{\text{RPA}}(\mathbf{k})$, and two-loop result (19), which are obvious, are thus fully explained in terms of magnon-magnon interactions.

2. Low-Temperature Thermodynamics

To gain further insight into the CA, we shall consider the low-temperature series for free energy comparing, where necessary, the prediction of CA with those of true magnon interaction theory[97]. Starting from the magnon Hamiltonian (9) on simple cubic lattice we obtain Hamiltonian density [66, 98] up to \mathbf{p}^6

$$\begin{aligned}
\mathcal{H}_0 &= \frac{F^2}{2} \partial_\alpha \pi \cdot \partial_\alpha \pi - \Sigma \mu H (1 - \pi^2/2), \\
\mathcal{H}^{[2]} &= \frac{F^2}{8} [\pi^2 \pi \cdot \Delta \pi - \pi^2 \Delta \pi^2] \\
&\quad + \frac{F^2}{32} \left[\pi^4 \Delta \pi^2 - \frac{1}{18} \pi^6 \Delta \pi^2 \right] \\
\mathcal{H}^{[4]} &= -l_1 \partial_\alpha^2 \pi \cdot \partial_\alpha^2 \pi \\
&\quad + \frac{l_1}{4} [\partial_\alpha^2 (\pi^2 \pi) \cdot \partial_\alpha^2 \pi - \partial_\alpha^2 \pi^2 \partial_\alpha^2 \pi^2] \\
&\quad + \frac{l_1}{16} \left[\partial_\alpha^2 \pi^4 \partial_\alpha^2 \pi^2 - \frac{1}{18} \partial_\alpha^2 \pi^6 \partial_\alpha^2 \pi^2 \right] \\
\mathcal{H}^{[6]} &= c_1 \partial_\alpha^3 \pi \cdot \partial_\alpha^3 \pi \\
&\quad + \frac{c_1}{4} [-\partial_\alpha^3 (\pi^2 \pi) \cdot \partial_\alpha^3 \pi + \partial_\alpha^3 \pi^2 \partial_\alpha^3 \pi^2] \\
&\quad + \frac{c_1}{16} \left[-\partial_\alpha^3 \pi^4 \partial_\alpha^3 \pi^2 + \frac{1}{18} \partial_\alpha^3 \pi^6 \partial_\alpha^3 \pi^2 \right],
\end{aligned} \tag{38}$$

with external magnetic field along z -axis, formal values of coupling constants $l_1 = F^2 a^2/24$, $c_1 = F^2 a^4/720$ and $\Delta = \partial_\alpha \partial_\alpha$. Given the Hamiltonian density (38) and knowing that the loops are suppressed by $D = 3$ powers of momentum (see (12)), we are in the position to set up a diagrammatic series for the free energy density $f = F/V$ [66, 99]. The magnon vertices in continuum field-theoretic setting will be marked by corresponding power of momentum with exception of those generated by $\mathcal{H}^{[2]}$, denoted by a dot.

The diagrams split into two categories [66]. The first one collects all one-loop diagrams with two-magnon vertices which describe lattice anisotropies. It is easy to see

that their contribution to the free energy of O(3) HFM on a simple cubic lattice yields terms whose powers of temperature are $5/2, 7/2, 9/2$ and so on. Moreover, the coefficients of two-magnon terms are the same in CA as in true magnon-interaction theory (compare (38) with equation (71) of [66]). It is therefore not surprising that CA exactly reproduces first three terms in low-temperature series for spontaneous magnetization [95], as they are a simple consequence of the lattice anisotropies.

Much more interesting are multiloop diagrams as they arise due to magnon-magnon interactions. Out of two-loop diagrams, the first one that describes the magnon-magnon interaction, and is a potential candidate for T^4 term, comes from four-magnon parts of $\mathcal{H}^{[2]}$. Yet, it vanishes since contributions from unimodular constraint and WZ term precisely cancel as in true magnon interaction theory [60, 61, 66]. The fact that low-temperature expansions obtained by Callen [95] do contain T^4 term for $S = 1/2$ should be ascribed to the pure artifact of TGF formalism [100]. Thus, the first nonzero contribution to the free energy arising solely from magnon-magnon interactions in CA is the Dyson term (proportional to T^5), the two-loop diagram of $\mathcal{H}^{[4]}$ [66]:

$$\begin{aligned}
\delta f_5 &= -T \text{ (diagram: two circles connected at a central square vertex labeled 4)} \\
&= -\frac{9l_1 \pi^3}{2\Sigma^2} \left(\frac{1}{2\pi}\right)^6 \left(\frac{\Sigma}{F^2}\right)^5 \left[\sum_{n=1}^{\infty} \frac{e^{-\mu H n/T}}{n^{5/2}} \right]^2 T^5.
\end{aligned} \tag{39}$$

The next two-loop diagram, including four-magnon vertex of $\mathcal{H}^{[6]}$ as well as two and four magnon vertices of $\mathcal{H}^{[4]}$ gives T^6 term (see [66]). Just as δf_5 , it occurs both in CA and in true magnon interaction theory. Still, this is not the leading correction to the Dyson term.

The next term describing magnon-magnon interactions comes from three-loop diagrams. In true magnon interaction theory, this is the three loop diagram of $\mathcal{H}^{[2]}$ [61, 66]

$$\begin{aligned}
\delta f_{11/2} &= -T \text{ (diagram: three circles connected at a central dot vertex)} = -\frac{1}{\Sigma^2} \left(\frac{\Sigma}{F^2}\right)^{9/2} I(h) T^{11/2}, \\
h &= \mu H/T,
\end{aligned} \tag{40}$$

where, in the absence of external magnetic field H , $I(h=0) = 5.3367 \times 10^{-6}$ [66]. As the analysis from previous section showed that the CA magnon dispersion emerges through the perturbation theory only if interactions described by two-vertex (and higher) diagrams are neglected [101], the CA low-temperature series for free energy does not contain $T^{11/2}$ term of (40). However, a term proportional to $T^{11/2}$ is present in CA, and it is generated by three-loop diagram of $\mathcal{H}^{[2]}$. Since

$$\text{(diagram: three circles connected at a central dot vertex)} = \text{(diagram: three circles connected at a central dot vertex with momenta p, q, Q)} + \text{(diagram: three circles connected at a central dot vertex with momenta p, q, Q)}, \tag{41}$$

with first colored contraction appearing four times and second one vanishing, we find

$$\delta f_{11/2}^{\text{CA}} = -\frac{2}{\Sigma^2} \left(\frac{\Sigma}{F^2} \right)^{9/2} \frac{\pi^{9/2}}{(2\pi)^9} \left[\sum_{n=1}^{\infty} \frac{e^{-\mu H n/T}}{n^{3/2}} \right]^2 \times \left[\sum_{n=1}^{\infty} \frac{e^{-\mu H n/T}}{n^{5/2}} \right] T^{11/2} \quad (42)$$

By comparing (40) and (42) for $H = 0$, we that CA overestimates the leading correction to Dyson's term nearly by a factor of 39. Obtaining expression (42) within TGF formalism is somewhat tedious, but rather straightforward within magnon perturbation theory, i.e. when appropriate set of magnon-magnon interactions have been identified.

Finally, we note that Hamiltonian (38) can be obtained from the Lagrangian

$$\mathcal{L} = \mathcal{L}^{[2]} + \mathcal{L}^{[4]} + \mathcal{L}^{[6]} \quad (43)$$

where

$$\begin{aligned} \mathcal{L}^{[2]} &= \Sigma \frac{\partial_t U^1 U^2 - \partial_t U^2 U^1}{1 + U^3} - \frac{F^2}{2} \partial_\alpha \mathbf{U} \cdot \partial_\alpha \mathbf{U} + \Sigma \mu H U^3 \\ &+ \frac{F^2}{32} \partial_\alpha \pi^4 \partial_\alpha \pi^2 - \frac{F^2}{576} \partial_\alpha \pi^6 \partial_\alpha \pi^2 \\ &- \frac{F^2}{128} \partial_\alpha \pi^4 \partial_\alpha \pi^4 + \frac{F^2}{128} \partial_\alpha (\pi^6 \pi) \cdot \partial_\alpha \pi, \end{aligned} \quad (44)$$

$$\begin{aligned} \mathcal{L}^{[4]} &= l_1 \partial_\alpha^2 \mathbf{U} \cdot \partial_\alpha^2 \mathbf{U} - \frac{l_1}{16} \left[\partial_\alpha^2 \pi^4 \partial_\alpha^2 \pi^2 - \frac{1}{18} \partial_\alpha^2 \pi^6 \partial_\alpha^2 \pi^2 \right] \\ &- \frac{l_1}{64} \left[\partial_\alpha^2 (\pi^6 \pi) \cdot \partial_\alpha^2 \pi - \partial_\alpha^2 \pi^4 \partial_\alpha^2 \pi^4 \right], \end{aligned} \quad (45)$$

$$\begin{aligned} \mathcal{L}^{[6]} &= c_1 \mathbf{U} \cdot \partial_\alpha^3 \partial_\alpha^3 \mathbf{U} - \frac{c_1}{16} \left[\pi^4 \partial_\alpha^3 \partial_\alpha^3 \pi^2 - \frac{1}{18} \pi^6 \partial_\alpha^3 \partial_\alpha^3 \pi^2 \right] \\ &- \frac{c_1}{64} \left[\pi^6 \pi \cdot \partial_\alpha^3 \partial_\alpha^3 \pi - \pi^4 \partial_\alpha^3 \partial_\alpha^3 \pi^4 \right], \end{aligned} \quad (46)$$

It is seen that each $\mathcal{L}^{[2]}$, $\mathcal{L}^{[4]}$ and $\mathcal{L}^{[6]}$ contain terms which manifestly violate internal symmetry of the Heisenberg model, just as in the case of RPA.

The explicit expressions from Sec. III D and Sec. III E should supplement imprecise statements relating RPA to CA found in the literature and dating as back as Callen's original paper [95]. For example, Tahir-Kheli introduces CA as an approximation which takes "into account the fluctuations of S_n^z around its average $\langle S^z \rangle$ " [102]. Further, it is claimed in a recent paper [93] that "CA takes, to some extent, account of magnon-magnon interactions", without actually specifying their type. Also, the point of view in standard and up-to-date reference on TGF method [12] is that CA "takes some higher-order correlations into account". By trying the issue of RPA/CA relationship down to the problem of magnon-magnon interactions, we have shown that effective Hamiltonians (i.e. Lagrangians) that generate RPA and CA through perturbation theory violate O(3) symmetry of the Heisenberg model at $\mathcal{O}(\mathbf{p}^2)$. A difference is, of course, that manifest symmetry breaking in CA takes place at six and eight magnon terms developing deviations from true magnon interaction theory at three-loop corrections to the free energy, while RPA breaks down already at two loop.

F. Comparison with quantum Monte Carlo simulation

We conclude the analysis in this section by comparing predictions of effective field theories for RPA and CA with quantum Monte Carlo (QMC) simulations and true magnon interaction theory for the O(3) ferromagnet free energy. This will allow us to infer the influence of RPA and CA-type magnon-magnon interactions on thermodynamics beyond leading order expansions in T discussed so far. The usefulness of the lattice EFT pursued here will become clear when we look at results away from low-temperature sector, i.e. when the lattice structure becomes resolved by magnons. While equations given bellow apply equally for arbitrary lattice, exchange integral J and localized spin S , all numerical calculations are conducted for the $S = 1/2$ Heisenberg ferromagnet on a simple cubic lattice with $J = 1$. The parameters $S = 1/2$ and $J = 1$, together with the lattice type, define a concrete realization of the Heisenberg ferromagnet. On the other hand, the parameters of EFT are F and Σ and are related to those of original Heisenberg Hamiltonian by matching [see the discussion bellow equation (11)].

The free energy (per lattice site) corresponding to the non-interacting theory is calculated with H_0 of (9). This is basically a LSW result and is given by

$$\frac{F_{\text{LSW}}}{N} = \frac{F_0}{N} + T v_0 \int_{\mathbf{k}} \ln \left[1 - e^{-\omega_0(\mathbf{k})/T} \right]. \quad (47)$$

To make comparison with QMC easier, we have normalized the non-interacting free energy by adding $F_0/N = -3/4$, the ground state energy of $S = 1/2$ and $J = 1$ Heisenberg ferromagnet on the simple cubic lattice. We note that F_{LSW} includes all one-loop diagrams (in the sense of derivative expansion) permitted by the lattice symmetry.

The two-loop correction to F_{LSW} in true magnon interaction theory (TMIT) is found in [66] to be

$$\frac{\delta F_{\text{TMIT}}}{N} = -\frac{1}{S} \frac{1}{2m_0} \frac{|\boldsymbol{\lambda}|^2}{4D} \left[v_0 \int_{\mathbf{p}} \langle n_{\mathbf{p}} \rangle_0 \widehat{\mathbf{p}}^2 \right]^2 \quad (48)$$

and the two-loop correction corresponding to RPA is

$$\begin{aligned} \frac{\delta F_{\text{RPA}}}{N} &= -T \text{RPA} \\ &= -\frac{1}{2S} \frac{v_0^2}{2m_0} \int_{\mathbf{p}, \mathbf{q}} \langle n_{\mathbf{p}} \rangle_0 \langle n_{\mathbf{q}} \rangle_0 \widehat{\mathbf{p} - \mathbf{q}}^2 \end{aligned} \quad (49)$$

with RPA vertex defined bellow equation (21). According to the discussion from Sec. III E, CA type of magnon-magnon interactions induce two, three and four-loop single vertex contributions to the ferromagnet free energy. While the two-loop term is the same as in TMIT [equation (48)], the three and four loop corrections are given

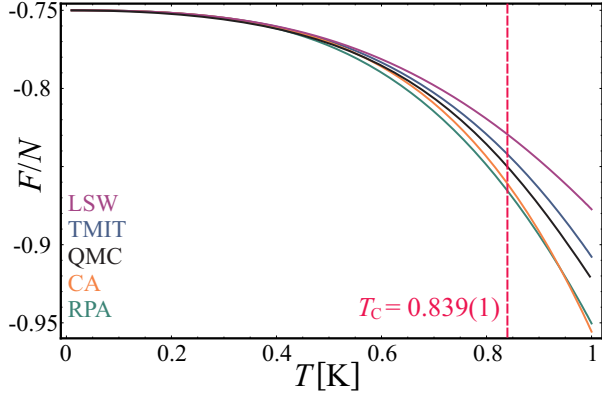


FIG. 3. The influence of magnon-magnon interactions on the free energy of $S = 1/2$ and $J = 1$ Heisenberg ferromagnet on the simple cubic lattice. The purple (top) curve represents the non-interacting model (LSW), while blue and black one represent TMIT and QMC results. The orange and green lines correspond to the models with interactions of CA and RPA type. The value of critical temperature $T_C = 0.839(1)$ K is taken from [105].

by

$$\begin{aligned} \frac{\delta F_{CA}^{3\text{loop}}}{N} &= -T \text{ (diagram with 6(b) loop)} \\ &= -\frac{1}{S^2} \frac{\langle n_{\mathbf{x}} \rangle}{2m_0} v_0^2 \int_{\mathbf{p}, \mathbf{q}} \langle n_{\mathbf{p}} \rangle_0 \langle n_{\mathbf{q}} \rangle_0 \widehat{\mathbf{p} - \mathbf{q}}^2 \quad (50) \end{aligned}$$

and

$$\begin{aligned} \frac{\delta F_{CA}^{4\text{loop}}}{N} &= -T \text{ (diagram with 8(c) loop)} \\ &= \frac{1}{2S^3} \frac{\langle n_{\mathbf{x}} \rangle^2}{2m_0} v_0^2 \int_{\mathbf{p}, \mathbf{q}} \langle n_{\mathbf{p}} \rangle_0 \langle n_{\mathbf{q}} \rangle_0 \widehat{\mathbf{p} - \mathbf{q}}^2. \quad (51) \end{aligned}$$

Finally, the simulation was performed using stochastic series expansion within quantum Wang-Landau algorithm [103] based on ALPS libraries [104]. The cutoff is set to 5×10^4 , which, for the SC lattice with 10^3 sites, yields reliable results if $T \gtrsim 0.05J$ (with $J = 1$). By letting the number of Wang-Landau refinement steps to be 18, the total number of sweeps becomes $\sim 10^{10}$ and the error bars are much smaller than the line used to display the simulation results.

Results of calculations are collected on Fig. 3. First, it is obvious that all lattice magnon models (including LSW) develop only small deviations from QMC almost up to $T = 0.5$ K. This clearly confirms our remarks about weakness of magnon-magnon interactions even in the case of $S = 1/2$ since the critical temperature is, from QMC simulations, known to be $T_C \approx 0.84$ K [105].

It is also evident that TMIT produces results closest to QMC in wide temperature range, as expected, demonstrating efficiency of the lattice magnon theory. Probably the most important observation concerning practical applications and interpretations of RPA and CA is that both approximations are based on interacting theories which, thanking the loop structure of corrections and corresponding Hamiltonians, *overestimate* the influence of magnon-magnon interactions [compare with equation (42)]. This is the main reason why self-consistent descriptions of real compounds based on RPA/CA, as a rule, predict higher values of the exchange integral J than LSW or non-linear spin-wave theories based on boson representations [106]. For example, the non-linear spin wave theory in combination with experimental data for 3D ferromagnet CrBr_3 predicts the intra- and inter-layer nearest neighbor exchange integrals $J = 8.25$ K and $J' = 0.497$ K [107]. In contrast, self-consistently determined exchange integrals within RPA are $J = 12.38$ K and $J' = 1.0$ K [8]. Of course, the strength of magnon-magnon interactions in RPA and CA at higher temperatures is masked by the special form of self-consistent equations for correlation functions. Namely, RPA and CA solutions in TGF formalism share many features with simple mean-field description at higher temperatures, exemplified by the expressions for the Curie temperature and the value of critical index β . As a result, both RPA and CA predict somewhat higher value for the critical temperature ($T_C^{\text{RPA}} \approx 0.989$ K and $T_C^{\text{CA}} \approx 1.326$ K for $J = 1$ and $S = 1/2$ ferromagnet on a simple cubic lattice). Finally, we note that the similar conclusions concerning low-temperature behavior of $\text{O}(3)$ ferromagnet at low temperatures were reached in [108].

IV. PERTURBATION THEORY FOR TYPE A MAGNONS

Now we turn to the perturbation theory for type A Goldstone bosons. Basic diagrammatic rules remain the same, but the definition of thermal propagator changes. Also, we shall need to include more than one lattice Laplacian per vertex as well as couplings beyond nearest neighbors. All this can be achieved within formalism of colored propagators described in Sec. III B.

A. Kondo-Yamaji Equations

The approximation of Kondo and Yamaji (KYA) represents an extension of the EOM method in the sense the linearizations are conducted in equations containing \ddot{S}_n^\pm . The long-range order parameter $\langle S^z \rangle$ does not explicitly enter the magnon dispersion, making this approach suitable for low-dimensional systems [43, 44]. It is also a starting point in further developments of TGF formalism [19–21, 44]. Here, the focus will be on one-dimensional ferromagnet. Strictly speaking, effective field theory is not directly applicable to one-dimensional $\text{O}(3)$ ferromagnet in the absence of external magnetic field, since magnons acquire nonperturbatively generated gap. How-

ever, a careful analysis from [64, 65, 109, 110] reveals that first few terms in low-temperature series for free energy are well defined even in case of zero external field, and KYA yields results in agreement with thermal Bethe-ansatz in this extreme low- T sector [111].

The Kondo-Yamaji equations (KYE) for magnon dispersion

$$\omega_{\text{KY}}(k) = J\{[1 - \cos ka][1 - \tilde{c}_1 + \tilde{c}_2 - 2\tilde{c}_1 \cos ka]\}^{1/2},$$

$$\tilde{c}_n = \tilde{W}v_0 \int_p \frac{\coth \frac{\omega_{\text{KY}}(p)}{2T}}{2\omega_{\text{KY}}(p)} \gamma(np)[1 - \gamma(p)], \quad (52)$$

with $\tilde{W} \approx 2J$ and $\tilde{c}_0 = 3/2$ at low temperatures, $\gamma(p)$ and \int_p given in (2) and (13) for $D = 1$, are derived from the assumption of vanishing long range order (LRO) [43]. It turns out that is extremely useful to exploit the constrain $\tilde{c}_0 = 3/2$ directly and to write KYA dispersion as

$$\omega_{\text{KY}}^2(k) = c^2 \hat{k}^2 - c^2 \hat{k}^2 [3\tilde{c}_0 - \tilde{c}_1] \quad (53)$$

$$+ \hat{k}^2 c^2 \frac{a^6 \tilde{W} v_0}{4} \int_p \frac{\coth \frac{\omega_{\text{KY}}(p)}{2T}}{2\omega_{\text{KY}}(p)} [\hat{p}^2]^3 + \hat{k}^2 \hat{k}^2 a^2 c^2 \tilde{c}_1,$$

$$c^2 = \frac{J^2 a^2}{2}.$$

We shall demonstrate bellow that KYE (52) i.e. (53), can be obtained from the effective Lagrangian description of a ferromagnet chain if $\Sigma = 0$ is set in (8). When $\Sigma = 0$ the effective Lagrangian must include a term with two temporal derivatives and it takes pseudo-Lorentzian form

$$\mathcal{L}_{\text{eff}} = \frac{F^2}{2} \partial_t U^i \partial_t U^i - \frac{\gamma^2}{2} \partial_x U^i \partial_x U^i, \quad (54)$$

where, as before, \mathbf{U} denotes the unit vector field and F^2 and γ^2 are constants satisfying $c^2 = \gamma^2/F^2$. In contemporary nomenclature, this Lagrangian describes the dynamics of type A Goldstone bosons [57, 69].

B. Hamiltonian and perturbation theory for NN lattice model

To develop the perturbation theory that yields KYE, we construct the lattice magnon Hamiltonian. Since the Lagrangian (54) contains $[\partial_t \mathbf{U}]^2$, the Hamiltonian cannot be obtained as in preceding sections. Instead, we follow [112] to get the interaction picture Hamiltonian. By putting it on a spatial lattice (chain), we find the free part

$$H_0 = \frac{v_0}{2} \sum_x \left[\frac{1}{F^2} \Pi^a \Pi^a - \gamma^2 \pi^a \nabla^2 \pi^a \right] \quad (55)$$

with (thermal) propagator

$$D_{ab}(x-y, \tau_x - \tau_y) \equiv \langle \text{T} \{ \pi^a(x, \tau_x) \pi^b(y, \tau_y) \} \rangle_0 \quad (56)$$

$$= \frac{\delta_{ab}}{\beta} \sum_{n=-\infty}^{\infty} \int_q \frac{e^{iq(x-y) - i\omega_n(\tau_x - \tau_y)}}{\omega_0^2(q) + \omega_n^2},$$

free-magnon dispersion

$$\omega_0(q) = c\sqrt{\hat{q}^2} \equiv c\hat{q}, \quad (57)$$

and nearest-neighbour (NN) interaction piece

$$H_{\text{int}} = -\frac{\gamma^2}{8} v_0 \sum_x \pi^2 \nabla^2 \pi^2 - \frac{F^2}{2} v_0 \sum_x [\boldsymbol{\pi} \cdot \partial_\tau \boldsymbol{\pi}]^2 \quad (58)$$

where π^a denotes the interaction picture magnon field and Π^a is the corresponding canonical momentum.

To calculate one-loop self energy for interaction (58) we use diagrammatic rules outlined in Sec. III B. While the action of ∇^2 on propagator lines merely introduces a factor of \hat{q}^2 for external or loop momenta, propagators with temporal derivatives must be handled with care [112]. We find

$$D_{ab}^\tau \equiv \langle \text{T} \{ \partial_{\tau_x} \pi^a(x, \tau_x) \pi^b(y, \tau_y) \} \rangle_0$$

$$= \frac{\delta_{ab}}{\beta} \sum_{n=-\infty}^{\infty} \int_q D_\tau(q, \omega_n) e^{iq(x-y) - i\omega_n(\tau_x - \tau_y)},$$

$$D_{ab}^{-\tau} \equiv \langle \text{T} \{ \pi^a(x, \tau_x) \partial_{\tau_y} \pi^b(y, \tau_y) \} \rangle_0 \quad (59)$$

$$= \frac{\delta_{ab}}{\beta} \sum_{n=-\infty}^{\infty} \int_q D_{-\tau}(q, \omega_n) e^{iq(x-y) - i\omega_n(\tau_x - \tau_y)},$$

$$D_{ab}^{\tau\tau} \equiv \langle \text{T} \{ \partial_{\tau_x} \pi^a(x, \tau_x) \partial_{\tau_y} \pi^b(y, \tau_y) \} \rangle_0$$

$$= \frac{\delta_{ab}}{\beta} \sum_{n=-\infty}^{\infty} \int_q D_{\tau\tau}(q, \omega_n) e^{iq(x-y) - i\omega_n(\tau_x - \tau_y)},$$

where

$$D_\tau(q, \omega_n) = -D_{-\tau}(q, \omega_n) = \frac{-i\omega_n}{\omega_0^2(q) + \omega_n^2}$$

$$D_{\tau\tau}(q, \omega_n) = \frac{-\omega_0^2(q)}{\omega_0^2(q) + \omega_n^2} \quad (60)$$

Using propagators listed in (59) together with (56) and action of lattice Laplacians, we obtain one-loop self energy

$$\tilde{\Sigma}(k, \omega) = \frac{\gamma^2}{c^2} v_0 \int_p \frac{\coth \frac{\omega_0(p)}{2T}}{2\omega_0(p)} [\omega_0^2(p) + \omega^2 - \omega_0^2(p-k)]$$

$$= \gamma^2 v_0 \int_p \frac{\coth \frac{\omega_0(p)}{2T}}{2\omega_0(p)} \left[\frac{a^2}{2} \hat{k}^2 \hat{p}^2 - \hat{k}^2 + \frac{\omega^2}{c^2} \right] \quad (61)$$

and thus

$$\tilde{\omega}^2(k) = \omega_0^2(k) - \tilde{\Sigma}(k) \quad (62)$$

$$= \hat{k}^2 c^2 \left[1 - F^2 v_0 \int_p \frac{\coth \frac{\omega_0(p)}{2T}}{2\omega_0(p)} \frac{a^2}{2} \hat{p}^2 \right]$$

where $\tilde{\Sigma}(k) \equiv \tilde{\Sigma}(k, \omega_0(k))$ is the on-shell self energy. If we set $F^2 = 3\tilde{W} \approx 6J$ and interpret (62) as a self-consistent equation for $\tilde{\omega}(k)$,

$$\tilde{\omega}^2(k) = c^2 \hat{k}^2 \left[1 - F^2 v_0 \int_p \frac{\coth \frac{\tilde{\omega}(p)}{2T}}{2\tilde{\omega}(p)} \frac{a^2}{2} \hat{p}^2 \right]$$

$$= c^2 \hat{k}^2 [1 - 3\tilde{c}_0], \quad (63)$$

we see that the lattice model (58) with NN coupling accounts only for the leading term in $\Sigma_{\text{KY}}(k)$ listed in (53). Obviously, the full KYA self energy can be obtained only with additional interactions in the one-loop approximation.

C. Perturbation theory for KYA model

1. Colored diagrams for NNN interaction

Two additional conventions will enable us to imbed next-nearest neighbor (NNN) interactions, as well as interactions containing more than one lattice Laplacian into the framework of colored diagrams. They will also make diagrammatic rules suitable for potential higher-loop calculations. First, propagators affected by $\nabla_{(2)}^2$ will be denoted by a double colored line. Second, the presence of $\nabla_{(2)}^2$ or ∇^2 will be represented by colored edges of the pentagon, which denotes a vertex. For example, typical interaction containing both $\nabla_{(2)}^2$ and NN Laplacian ∇^2 is $V = v_0 \sum_x (\boldsymbol{\pi} \cdot \nabla_{(2)}^2 \boldsymbol{\pi})(\nabla^2 \boldsymbol{\pi} \cdot \nabla^2 \boldsymbol{\pi})$. Four distinct colored contractions contribute to one-loop self energy generated by V . These are

$$\begin{aligned}
 & \text{Diagram 1: } = -4v_0 \int_p \frac{\coth \frac{\omega_0(p)}{2T}}{2\omega_0(p)} \widehat{k}^2 \widehat{p}^2 \widehat{2p}^2, \\
 & \text{Diagram 2: } = -4v_0 \int_p \frac{\coth \frac{\omega_0(p)}{2T}}{2\omega_0(p)} \widehat{2k}^2 \widehat{p}^2 \widehat{p}^2, \\
 & \text{Diagram 3: } = -4v_0 \int_p \frac{\coth \frac{\omega_0(p)}{2T}}{2\omega_0(p)} \widehat{2k}^2 \widehat{k}^2 \widehat{p}^2, \quad (64) \\
 & \text{Diagram 4: } = -4v_0 \int_p \frac{\coth \frac{\omega_0(p)}{2T}}{2\omega_0(p)} \widehat{k}^2 \widehat{k}^2 \widehat{2p}^2.
 \end{aligned}$$

since each of diagrams listed above appears four times.

2. KYA self-energy

As a first step, we introduce the second-neighbor couplings in (55) and (58) by the replacement $\nabla^2 \rightarrow \nabla^2 - G^2 \nabla^4$, where

$$\nabla^4 := \nabla^2 \nabla^2 = \frac{4}{a^2} \left[\nabla_{(2)}^2 - \nabla^2 \right], \quad (65)$$

$\nabla_{(2)}^2$ being defined in (5) and the strength of the next-nearest neighbor (NNN) coupling G will be determined in perturbative expansion. Much of the results obtained for the NN model still hold. In particular, the propagator and the one-loop self energy retain their general form given in (56) and the first line of (61), respectively, with free dispersion being

$$\Omega_0^2(k) = c^2 \left[\widehat{k}^2 + G^2 \widehat{k}^2 \widehat{k}^2 \right], \quad c^2 = \gamma^2 / F^2. \quad (66)$$

Further, let us now introduce additional interaction terms

$$\begin{aligned}
 H_{\text{int}}^{(2)} &= K^{(2)} c^2 v_0 \sum_x (\boldsymbol{\pi} \cdot \nabla^4 \boldsymbol{\pi})(\nabla^2 \boldsymbol{\pi} \cdot \nabla^2 \boldsymbol{\pi}) \\
 H_{\text{int}}^{(3)} &= K^{(3)} c^2 v_0 \sum_x (\nabla^2 \boldsymbol{\pi} \cdot \nabla^2 \boldsymbol{\pi})(\nabla^2 \boldsymbol{\pi} \cdot \nabla^2 \boldsymbol{\pi}) \\
 H_{\text{int}}^{(4)} &= A c^2 v_0 \sum_x \boldsymbol{\pi} \cdot \nabla^2 \boldsymbol{\pi} \\
 H_{\text{int}}^{(5)} &= B c^2 v_0 \sum_x \boldsymbol{\pi} \cdot \nabla^4 \boldsymbol{\pi}
 \end{aligned} \quad (67)$$

where $H_{\text{int}}^{(3)}$ and $H_{\text{int}}^{(4)}$ serve as counter-terms, i.e. they absorb renormalizations of ∇^2 and ∇^4 couplings.

Individual contributions of (67) to the self-energy are evaluated using colored diagrams, as outlined above. To remain within KYA, we discard a term proportional to $\widehat{k}^2 \widehat{k}^2 \widehat{k}^2$ and arrange the remaining ones in two groups: the ones proportional to \widehat{k}^2 and those proportional to $\widehat{k}^2 \widehat{k}^2$. The corresponding self-consistent equation for magnon energy reduces to KYA form (53) if $A = 251/48$, $B + G^2 = 6a^2 \widetilde{c}_0$, $K^{(2)} = a^6 \widetilde{W}/16$, $K^{(3)} = -7a^6 \widetilde{W}/64$, $F^2 G^2 = a^2 \widetilde{W}/8$ and $\gamma^2 = c^2 F^2$. From the compact form of magnon energies [equation (52)], one readily shows that $\widetilde{c}_1 = \widetilde{c}_2 = 1/2$ at $T = 0$ K so that the magnon dispersion becomes identical with standard LSW result, $\omega(k) = J(a^2/2) \widehat{k}^2$. This is to be compared with $\Omega_0 \propto k$. Thus, in contrast to the perturbation theories for type B magnons from preceding section, interactions substantially change the magnon dispersion law in the present case. The possibility that interactions between Goldstone bosons may have such a strong impact on the geometry of their dispersion was anticipated only recently [113]. To the best of author's knowledge, calculations from this section offer the first explicit realization of such a mechanism. At finite temperatures, we find

$$\begin{aligned}
 \widetilde{c}_1 &\approx \frac{1}{2} - \frac{3I_{3/2}}{2} T^{\frac{3}{2}} - 2T^2, \quad \widetilde{c}_2 \approx \frac{1}{2} - \frac{9I_{3/2}}{2} T^{\frac{3}{2}} + 2T^2, \\
 I_{3/2} &= \frac{\zeta(3/2)}{\sqrt{2\pi}},
 \end{aligned} \quad (68)$$

leading to

$$\omega^2(k) \approx 4J^2 a^2 T^2 k^2 + \frac{J^2 a^4}{4} \left[1 - 3I_{3/2} T^{\frac{3}{2}} \right] k^4 \quad (69)$$

in agreement with [43].

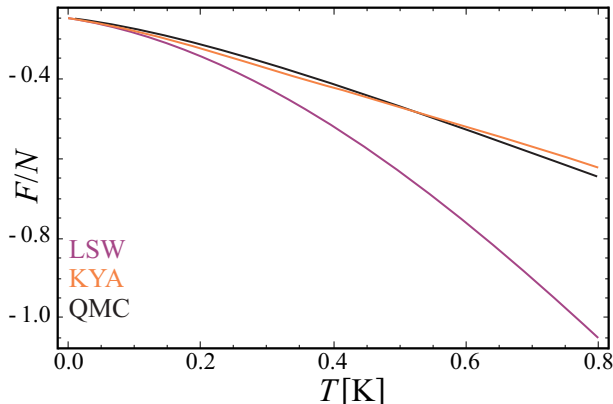


FIG. 4. The influence of interactions on the free energy of $S = 1/2$ and $J = 1$ Heisenberg ferromagnet on the chain lattice. The purple curve represents the standard non-interacting model (LSW), while the black one denotes QMC results. The orange line corresponds to the model with interactions of KYA type.

3. KYA Thermodynamics and Quantum Monte Carlo Simulation

Now we discuss the low-temperature series for free energy in self-consistent KYA. According to (69) and (54), magnon fields admit standard type A Fourier decomposition including both creation and annihilation operators which produces so-called zero-point term in expression for free energy [99]. The zero-point term is temperature dependent in the present case [see (52)] and, since there are two type A magnons, we find

$$\frac{F_{\text{KY}}^0}{N} = \frac{F_0}{N} + Tv_0 \int_p \ln [1 - e^{-\omega_0(p)/T}] + v_0 \int_p \omega_{\text{KY}}(p), \quad (70)$$

where $F_0/N = -5/4$ provides a proper normalization at $T = 0\text{K}$. To see that (53) indeed reproduces all main features of low-temperature series for free energy in KYA, we calculate (70) with the full Kondo-Yamaji dispersion [43] and the approximate one [equation (53) and solutions (68)]. The first two terms of these series match completely. While the first one, proportional to $T^{3/2}$, is rather expected [114], the second one is proportional to T^2 and describes the effects of interactions. The T^2 term is twice the one obtained by thermodynamic Bethe ansatz equations [115] since KYA describes $O(3)$ ferromagnet in terms of type-A magnons (a similar problem with T^2 term arises in SBMFT [7]). The direct application of TGF method yields $(7/3)T^2$ [111] instead of $2T^2$ and this discrepancy may be classified as another artifact of TGF formalism.

To check the validity of KYA result for free energy of a $S = 1/2$ ferromagnetic chain at arbitrary temperatures, we test it against QMC simulation. The simulation was conducted using Wang-Landau algorithm and ALPS libraries [104]. Results reliable up to $T \approx 0.01\text{K}$ are obtained by setting the cutoff at 3×10^4 .

The results shown at Fig. 4 compare KYA [equation (70)] to LSW and QMC. We see that, in contrast to naive LSW, KYA result agrees with QMC rather well in wide temperature range. Further, the present exposition reveals the mechanism behind KYA: similarly to RPA, magnon-magnon interactions generated by WZ term do not contribute to KYA. Instead, the dynamics of a ferromagnetic chain is governed by NN and NNN couplings for type A magnons, combined in a such manner that one-loop corrections yield spectrum usually encountered at type B systems at $T = 0$. Even though the KYA deviates from QMC only slightly, which makes it a relatively good method for qualitative description of a $S = 1/2$ ferromagnet chain, it introduces spurious terms arising from magnon-magnon interactions in the low-temperature series for free energy already at leading order, i.e. at T^2 [65, 115].

V. SUMMARY

Linearization of equations of motion (EOM) for spin operators is a popular and important tool for studying magnetic systems. These include not only insulating materials with localized spins but also itinerant electron systems where Heisenberg Hamiltonian arises through a mapping on an effective model. If the parameters of linearization are chosen carefully, i.e. if an appropriate "decoupling scheme" is used, this method will provide reliable results in many cases. For instance, solutions obtained with standard linearizations obey Mermin-Wagner theorem and agree with Monte Carlo simulations and experimental results. However, in choosing parameters of linearization one must rely on physical intuition since approximations are not controlled perturbatively (equations of motion contain the Heisenberg-picture spin operators) nor do magnon operators appear at any stage, so all linearizations are generally considered to be *ad hoc*. This raises several questions concerning proper interpretation of results obtained by EOM. For example, it is hard to identify types of interactions generated by various linearizations and their influence on thermodynamic properties, or to separate interaction-induced effects from those related to the choice of dynamical degrees of freedom. Because complete understanding of EOM method is a prerequisite for its successful application, these issues need to be resolved.

On the other hand, effective field theory (EFT) is a powerful tool for handling dynamics of Goldstone particles as it provides systematic (and model independent) method for describing interaction effects. From this point of view, $O(3)$ ferromagnet is a rather interesting system since magnon-magnon interactions come in two categories: the ones induced by the unimodular constrain and those generated by the Wess-Zumino (WZ) term. The main advantage of EFT over EOM is that magnon-magnon interaction terms appear explicitly in the Hamiltonian (Lagrangian) making the dynamics of magnons completely unrelated to the local $su(2)$ algebra of spin operators that define the Heisenberg Hamiltonian.

The present paper deals with interaction effects in-

duced by the three most commonly used linearizations: random phase approximation (RPA), Callen approximation (CA) and Kondo-Yamaji approximation (KYA). It is shown that all unique properties of linearizations mentioned above originate in different treatments of WZ term, where type B (A) magnons are described by the model with (without) WZ term. Since all linearizations discussed in the present paper respect discrete structure of the Heisenberg Hamiltonian, we employ lattice regularization that preserves these symmetries. Perturbative calculations are conducted with the aid of colored diagrams which are particularly suited for theories with derivative couplings.

As the simplest of type B models, RPA describes the O(3) ferromagnet with one-loop interaction theory in such way that interactions specific to the WZ term are neglected [see Sec. III D]. This simplification induces violation of O(3) symmetry at leading interaction terms of order \mathbf{p}^2 and eventually produces spurious terms in low-temperature series for free energy. Even though the O(3) symmetry is explicitly broken by interaction terms in effective Hamiltonian, the constrain $v_0 \int_{\mathbf{p}} \hat{\mathbf{p}}^2 \langle n_{\mathbf{p}} \rangle_0 = 0$ in the one-loop self energy eliminates the gap at the same time introducing site independent average number of magnons. Thus, opposed to some claims found in the literature [see the discussion in the last paragraph of Sec. III D], magnon-magnon interactions are accounted for in RPA. These are interactions induced by the unimodular constrain, i.e. they are generated by the geometry of coset space $O(3)/O(2) = S^2$.

The next approximation considered in the text is CA, viewed by many as an improvement over RPA. Unfortunately, the claims of superiority of CA over RPA have been supported only by some vague statements concerning additional correlations or interactions induced by this linearization scheme [see the discussion at the ending of Sec. III E 2], or by a subsequent analysis of low-temperature series for spontaneous magnetization. However, *a posteriori* analysis of low-temperature series can not distinguish between interaction effects and pure artifacts of the formalism and therefore it can not be considered as a complete one. In contrast, analysis based on the effective field theory presented in Sec. III E reveals that, regarding magnon-magnon interactions, CA does contain certain improvements over RPA. Concretely, four magnon interactions arising from WZ term appear in CA through one-loop corrections in the magnon self-energy [see Sec. III E 1]. However, additional spurious six and eight magnon interaction terms included in CA violate O(3) symmetry at \mathbf{p}^2 through two and three loop corrections to the self energy. Therefore, the constrain $v_0 \int_{\mathbf{p}} \hat{\mathbf{p}}^2 \langle n_{\mathbf{p}} \rangle_0 = 0$ must be imposed on those contributions to the self energy that arise from symmetry violating terms, just as it is in RPA. Also, one should note that all corrections to the self energy in CA come from one-vertex diagrams. Because of that, magnon energies

in CA, as well as in RPA, possess the same geometry as LSW solution (that is, $\omega(\mathbf{k}) \propto \hat{\mathbf{k}}^2$). Alternatively, as described in Sec. III E 2, magnon-magnon interactions induced by WZ term and unimodular constrain constitute two-loop corrections to the free energy in CA which gives correct results at order T^5 (this is the leading term in low-temperature series generated by interactions). However, symmetry violating terms produce deviation from true magnon interaction theory at order $T^{11/2}$ (that is, at three-loop corrections to the free energy).

In addition, the applicability of lattice field theories for type B magnons in wide temperature range is demonstrated by comparison with quantum Monte Carlo (QMC) simulation [see Sec. III F]. Excellent agreement between QMC and LSW theory combined with one-loop correction to the free energy [equations (47) and (48)] additionally supports lattice EFT as a right method for interpretation of EOM results.

Further, we discuss KYA and show that its physics near $T = 0\text{K}$ can be reduced to the self-consistent perturbation theory for type A magnons. Therefore, WZ term and magnon-magnon interactions that it generates do not enter KYA, making this approximation substantially different from RPA and CA. Still, at $T = 0\text{K}$, KYA reproduces standard dispersion for ferromagnetic magnons, $\omega(\mathbf{k}) \propto \hat{\mathbf{k}}^2$. This property of KYA is usually explained with phenomenological vertex parameters which account spin-spin correlations and maintain rotational invariance. In Sec. IV we show that these characterizations of KYA may be replaced with self-consistent one-loop perturbation theory for a model of type A magnons with explicit identification of interaction terms. In particular, KYA Hamiltonian contains lattice Laplacians that connect first as well as second neighbors on a chain lattice and these additional interactions play a key role in producing characteristic dispersion at $T = 0\text{K}$. Analysis of the free energy reveals that KYA low-temperature series for free energy deviates from rigorous results already at leading term which is a consequence of interactions. However, at the same time, KYA result differs from QMC only slightly in wide temperature range [section IV C 3] and provides qualitative description of the low-temperature thermodynamics.

A detailed analysis based on lattice magnon fields presented in the paper revealed physics behind RPA, CA and KYA in case of O(3) ferromagnets. All three approximations are reduced to equivalent systems of interacting magnons thus providing better understanding of widely used theoretical tools.

ACKNOWLEDGEMENT

This work was supported by the Serbian Ministry of Education and Science under Grant No. OI 171009.

[1] M. E. Zhitomirsky and A. L. Chernyshev, *Rev. Mod. Phys.* **85**, 219 (2013).

[2] E. Dagotto, *Rev. Mod. Phys.* **66**, 763 (1994).

- [3] M. Imada, A. Fujimori, and Y. Tokura, *Rev. Mod. Phys.* **70**, 1039 (1998).
- [4] G. R. Stewart, *Rev. Mod. Phys.* **83**, 1589 (2011).
- [5] D. C. Johnston, *Adv. Phys.* **59**, 803 (2010).
- [6] S. Weinberg, in *Conceptual Foundations of Quantum Field Theory*, edited by T. Y. Cao (Cambridge University Press, 2004).
- [7] A. Auerbach, *Interacting Electrons and Quantum Magnetism* (Springer-Verlag, 1994).
- [8] V. Y. Irkhin, A. A. Katanin, and M. I. Katsnelson, *Phys. Rev. B* **60**, 1082 (1999).
- [9] J. Otsuki and Y. Kuramoto, *Phys. Rev. B* **88**, 024427 (2013).
- [10] F. Englert, *Phys. Rev. Lett.* **5**, 102 (1960).
- [11] G. S. Guralnik and C. R. Hagen, and T. W. B. Kibble, in *Advances in Particle Physics*, Vol. 2, edited by R. L. Cool and R. E. Marshak (Wiley, 1968).
- [12] P. Frbrich and P. Kuntz, *Phys. Repts.* **432**, 223 (2006).
- [13] M. Manojlović, M. Pavkov, M. Škrinjar, M. Pantić, D. Kapor, and S. Stojanović, *Phys. Rev. B* **68**, 014435 (2003).
- [14] M. S. Rutonjski, S. M. Radošević, M. G. Škrinjar, M. V. Pavkov-Hrvojević, D. V. Kapor, and M. R. Pantić, *Phys. Rev. B* **76**, 172506 (2007).
- [15] S. Radošević, M. Pavkov-Hrvojević, M. Pantić, M. Rutonjski, D. Kapor, and M. Škrinjar, *Eur. Phys. J. B* **68**, 511 (2009).
- [16] M. S. Rutonjski, S. M. Radošević, M. R. Pantić, M. V. Pavkov-Hrvojević, D. V. Kapor, and M. G. Škrinjar, *Solid State Commun.* **151**, 518 (2011).
- [17] S. M. Radošević, M. S. Rutonjski, M. R. Pantić, M. V. Pavkov-Hrvojević, D. V. Kapor, and M. G. Škrinjar, *Solid State Commun.* **151**, 1753 (2011).
- [18] E. Sasoglu, L. Sandratskii, P. Bruno, and I. Galanakis, *Phys. Rev. B* **72**, 184415 (2005).
- [19] I. Junger, D. Ihle, J. Richter, and A. Klümper, *Phys. Rev. B* **70**, 104419 (2004).
- [20] I. J. Junger, D. Ihle, and J. Richter, *Phys. Rev. B* **72**, 064454 (2005).
- [21] M. Härtel, J. Richter, O. Götze, D. Ihle, and S.-L. Drechsler, *Phys. Rev. B* **87**, 054412 (2013).
- [22] J. Kudrnovský, V. Drchal, L. Bergqvist, J. Rusz, I. Turek, B. Újfalussy, and I. Vincze, *Phys. Rev. B* **90**, 134408 (2014).
- [23] D. Yamamoto and S. Kurihara, *Phys. Rev. B* **75**, 134520 (2007).
- [24] S. Henning, F. Körmann, J. Kienert, W. Nolting, and S. Schwieger, *Phys. Rev. B* **75**, 214401 (2007).
- [25] T. N. Antsygina, M. I. Poltavskaya, I. I. Poltavsky, and K. A. Chishko, *Phys. Rev. B* **77**, 024407 (2008).
- [26] D. Yamamoto, S. Todo, and S. Kurihara, *Phys. Rev. B* **78**, 024440 (2008).
- [27] H.-Y. Wang, *Phys. Rev. B* **86**, 144411 (2012).
- [28] D. A. Yablonskiy, *Phys. Rev. B* **44**, 4467 (1991).
- [29] M. A. Fayzullin, R. M. Eremina, M. V. Eremin, A. Dittl, N. van Well, F. Ritter, W. Assmus, J. Deisenhofer, H.-A. K. von Nidda, and A. Loidl, *Phys. Rev. B* **88**, 174421 (2013).
- [30] D. Schmalfuß, R. Darradi, J. Richter, J. Schulenburg, and D. Ihle, *Phys. Rev. Lett.* **97**, 157201 (2006).
- [31] M. R. Pantić, D. V. Kapor, S. M. Radošević, and P. M. Mali, *Solid State Commun.* **182**, 55 (2014).
- [32] A. Vladimirov, D. Ihle, and N. Plakida, *Eur. Phys. J. B* **87**, 112 (2014), [10.1140/epjb/e2014-50152-y](https://doi.org/10.1140/epjb/e2014-50152-y).
- [33] L. S. Campana, L. De Cesare, U. Esposito, M. T. Mercaldo, and I. Rabuffo, *Phys. Rev. B* **82**, 024409 (2010).
- [34] J. F. Devlin, *Phys. Rev. B* **4**, 136 (1971).
- [35] M. Mercaldo, I. Rabuffo, L. Cesare, and A. Caramico DAuria, *The Eur. Phys. J. B* **86**, 1 (2013).
- [36] K. Sato, L. Bergqvist, J. Kudrnovský, P. H. Dedrichs, O. Eriksson, I. Turek, B. Sanyal, G. Bouzerar, H. Katayama-Yoshida, V. A. Dinh, T. Fukushima, H. Kizaki, and R. Zeller, *Rev. Mod. Phys.* **82**, 1633 (2010).
- [37] A. Chakraborty, P. Wenk, R. Bouzerar, and G. Bouzerar, *Phys. Rev. B* **86**, 214402 (2012).
- [38] T. Meng and D. Loss, *Phys. Rev. B* **87**, 235427 (2013).
- [39] K. L. Livesey and R. L. Stamps, *Phys. Rev. B* **81**, 064403 (2010).
- [40] S. Wang, R. Li, H.-H. Fu, L. Ding, and K. Yao, *Appl. Phys. Lett.* **103**, 132911 (2013).
- [41] M. Pajda, J. Kudrnovský, I. Turek, V. Drchal, and P. Bruno, *Phys. Rev. B* **64**, 174402 (2001).
- [42] I. Turek, J. Kudrnovsk, V. Drchal, and P. Bruno, *Philosophical Magazine* **86**, 1713 (2006), <http://dx.doi.org/10.1080/14786430500504048>.
- [43] J. Kondo and K. Yamaji, *Prog. Theor. Phys.* **47**, 807 (1972).
- [44] H. Shimahara and S. Takada, *J. Phys. Soc. Japan* **60**, 2394 (1991).
- [45] H. Leutwyler, *Phys. Rev. D* **49**, 3033 (1994).
- [46] S. Weinberg, *Phys. Rev.* **166**, 1568 (1968).
- [47] S. Coleman, J. Wess, and B. Zumino, *Phys. Rev.* **177**, 2239 (1969).
- [48] C. G. Callan, S. Coleman, J. Wess, and B. Zumino, *Phys. Rev.* **177**, 2247 (1969).
- [49] S. Weinberg, *Physica A* **96**, 327 (1979).
- [50] J. Gasser and H. Leutwyler, *Ann. Phys.* **158**, 142 (1984).
- [51] P. Gerber and H. Leutwyler, *Nucl. Phys. B* **321**, 387 (1989).
- [52] H. Leutwyler, *Ann. Phys.* **235**, 165 (1994).
- [53] S. Weinberg, *The Quantum Theory of Fields, Vol. II* (Cambridge University Press, 2010).
- [54] C. Burgess, *Phys. Repts.* **330**, 193 (2000).
- [55] T. B. Brauner, *Symmetry* **2**, 609 (2010).
- [56] J. M. Román and J. Soto, *Int. J. Mod. Phys. B* **13**, 755 (1999).
- [57] H. Watanabe and H. Murayama, *Phys. Rev. X* **4**, 031057 (2014).
- [58] J. Andersen, T. Brauner, C. Hofmann, and A. Vuorinen, *Journal of High Energy Physics* **2014**, 88 (2014), [10.1007/JHEP08\(2014\)088](https://doi.org/10.1007/JHEP08(2014)088).
- [59] C. P. Hofmann, *Phys. Rev. B* **60**, 388 (1999).
- [60] C. P. Hofmann, *Phys. Rev. B* **65**, 094430 (2002).
- [61] C. P. Hofmann, *Phys. Rev. B* **84**, 064414 (2011).
- [62] C. P. Hofmann, *Phys. Rev. B* **86**, 054409 (2012).
- [63] C. P. Hofmann, *Phys. Rev. B* **86**, 184409 (2012).
- [64] C. P. Hofmann, *Phys. Rev. B* **87**, 184420 (2013).
- [65] C. P. Hofmann, *Physica B: Condensed Matter* **442**, 81 (2014).
- [66] S. M. Radošević, M. R. Pantić, M. V. Pavkov-Hrvojević, and D. V. Kapor, *Ann. Phys.* **339**, 382 (2013).
- [67] M. I. Kaganov and A. V. Chubukov, *Sov. Phys. Uspekhi* **30**, 1015 (1987).
- [68] M.I. Kaganov and A.V. Chubukov, in *Spin Waves and Magnetic Excitations*, Modern Problems in Condensed Matter Sciences, Vol. 22, Issue 1, edited by A.S. Borovik-Romanov and S.K. Sinha (Elsevier, 1988) pp. 1 – 80.
- [69] H. Watanabe and H. Murayama, *Phys. Rev. Lett.* **108**, 251602 (2012).
- [70] C.-K. Chow, *Nucl. Phys. B* **547**, 281 (1999).

- [71] A. Jevicki and N. Papanicolaou, *Ann. Phys.* **120**, 107 (1979).
- [72] J. R. Klauder, *Phys. Rev. D* **19**, 2349 (1979).
- [73] B. Schlittgen and U.-J. Wiese, *Phys. Rev. D* **63**, 085007 (2001).
- [74] X. G. Wen and A. Zee, *Phys. Rev. Lett.* **61**, 1025 (1988).
- [75] T. Brauner and S. Moroz, *Phys. Rev. D* **90**, 121701 (2014).
- [76] S. Weinberg, *The Quantum Theory of Fields, Vol. I* (Cambridge University Press, 2008).
- [77] P. Hasenfratz and H. Leutwyler, *Nuclear Physics B* **343**, 241 (1990).
- [78] J. Gasser and H. Leutwyler, *Nucl. Phys. B* **307**, 763 (1988).
- [79] I. A. Shushpanov and A. V. Smilga, *Phys. Rev. D* **59**, 054013 (1999).
- [80] R. Lewis and P.-P. A. Ouimet, *Phys. Rev. D* **64**, 034005 (2001).
- [81] F. J. Dyson, *Phys. Rev.* **102**, 1217 (1956).
- [82] F. J. Dyson, *Phys. Rev.* **102**, 1230 (1956).
- [83] S.V. Maleev, *Sov. Phys. JETP* **6**, 776 (1958).
- [84] Originally, Dyson obtained Hamiltonian from the requirement that certain combination of boson operators has the same effect on ideal spin-wave states as the Heisenberg Hamiltonian does on spin-wave states (See [81] for Dyson's definitions of the spin-wave states). The Dyson Hamiltonian is also a direct consequence of the Dyson-Maleev [83] boson representation of spin operators.
- [85] To be precise, the weakness of magnon-magnon interactions is a characteristic of spin systems with collinear order, see [1].
- [86] Ferromagnetic magnons are massless from the point of the view of the Goldstone theorem, but giving the non-relativistic form of the dispersion (See (13)), it is convenient to refer to m_0 and $m(T)$ as magnon mass.
- [87] J. Gasser and H. Leutwyler, *Nucl. Phys. B* **250**, 465 (1985).
- [88] R. Stinchcombe, G. Horwitz, F. Englert, and R. Brout, *Phys. Rev.* **130**, 155 (1963).
- [89] V. Vaks, A. Larkin, and S. Pikin, *Sov. Phys. JETP* **26**, 188 (1968).
- [90] V. Vaks, A. Larkin, and S. Pikin, *Soviet Physics JETP* **26**, 647 (1968).
- [91] R. S. Fishman and G. Vignale, *Phys. Rev. B* **44**, 658 (1991).
- [92] F.-s. Liu, Z. Wang, W.-f. Chen, and X.-j. Yuan, *Phys. Rev. B* **51**, 12491 (1995).
- [93] R. Bastardis, U. Atxitia, O. Chubykalo-Fesenko, and H. Kachkachi, *Phys. Rev. B* **86**, 094415 (2012).
- [94] A. Vladimirov, D. Ihle, and N. Plakida, *Theor. Math. Phys.* **177**, 1540 (2013).
- [95] H. B. Callen, *Phys. Rev.* **130**, 890 (1963).
- [96] X. G. Wen, *Quantum Field Theory of Many Body Systems* (Oxford University Press, 2007).
- [97] The accompanying analysis of low-temperature thermodynamics in the RPA model, defined in Sec. IIID, can be found in [66].
- [98] T. Dombre and N. Read, *Phys. Rev. B* **38**, 7181 (1988).
- [99] J. I. Kapusta and C. Gale, *Finite-Temperature Field Theory - Principles and Applications* (Cambridge University Press, 2006).
- [100] Actually, Callen found corresponding spurious T^3 term in low-temperature series for spontaneous magnetization and not directly the T^4 term discussed here.
- [101] This does not exclude multi-vertex diagrams if all except single vertex describe lattice anisotropies.
- [102] R. A. Tahir-Kheli, *Phys. Rev.* **132**, 689 (1963).
- [103] M. Troyer, S. Wessel, and F. Alet, *Phys. Rev. Lett.* **90**, 120201 (2003).
- [104] B. Bauer, L. D. Carr, H. G. Evertz, A. Feiguin, J. Freire, S. Fuchs, L. Gamper, J. Gukelberger, E. Gull, S. Guertler, A. Hehn, R. Igarashi, S. V. Isakov, D. Koop, P. N. Ma, P. Mates, H. Matsuo, O. Parcollet, G. Pawłowski, J. D. Picon, L. Pollet, E. Santos, V. W. Scarola, U. Schollwöck, C. Silva, B. Surer, S. Todo, S. Trebst, M. Troyer, M. L. Wall, P. Werner, and S. Wessel, *Jour. Stat. Mech.* **2011**, P05001 (2011).
- [105] S. Wessel, *Phys. Rev. B* **81**, 052405 (2010).
- [106] In a self-consistent description of particular compound, modeled by a Heisenberg Hamiltonian, all microscopic parameters such as the exchange integral J are determined by matching with experimental data for some physical quantity.
- [107] H. Davis and A. Narath, *Phys. Rev.* **134**, A433 (1964).
- [108] M. Correggi, A. Giuliani, and R. Seiringer, *Europhys. Lett.* **108**, 20003 (2014).
- [109] M. Takahashi, *Progr. of Theor. Phys. Suppl.* **87**, 233 (1986).
- [110] M. Takahashi, *Phys. Rev. Lett.* **58**, 168 (1987).
- [111] T. Koma, *Prog. of Theor. Phys.* **81**, 783 (1989).
- [112] I. S. Gerstein, R. Jackiw, B. W. Lee, and S. Weinberg, *Phys. Rev. D* **3**, 2486 (1971).
- [113] H. Watanabe and T. Brauner, *Phys. Rev. D* **84**, 125013 (2011).
- [114] The $T^{3/2}$ term is also found using thermodynamic Bethe ansatz equations [115], effective field theory [64], Schwinger boson mean field theory (SBMFT) [7] and LSW.
- [115] M. Takahashi and M. Yamada, *J. Phys. Soc. Jpn.* **54**, 2808 (1985).